Faculty of Aerospace Engineering

Increasing Acceptance of Tactile Feedback in UAV Teleoperations by Visualizing Force Fields

V. Ho

October 10, 2016

Delft University of Technology

Challenge the future

Increasing Acceptance of Tactile Feedback in UAV Teleoperations by Visualizing Force Fields

Master of Science Thesis

For obtaining the degree of Master of Science in Aerospace Engineering
at Delft University of Technology

V. Ho

October 10, 2016

Faculty of Aerospace Engineering · Delft University of Technology

Delft University of Technology

Delft University Of Technology
Department Of
Control and Simulation

The undersigned hereby certify that they have read and recommend to the Faculty of Aerospace Engineering for acceptance a thesis entitled **"Increasing Acceptance of Tactile Feedback in UAV Teleoperations by Visualizing Force Fields"** by **V. Ho** in partial fulfillment of the requirements for the degree of **Master of Science**.

Dated: October 10, 2016

Readers:

____
prof.dr.ir. M. Mulder

____
dr.ir. C. Borst

____
dr.ir. M. M. van Paassen

____
dr.ir. W. Mugge

Acronyms

ACC	Adaptive Cruise Control
CAF	Circular Avoidance Field
CARS	Controller Acceptance Rating Scale
DUECA	Delft University Environment for Communication and Activation
EID	Ecological Interface Design
LoA	Level of Automation
NASA-TLX	NASA Task Load Index
ND	Navigation Display
OBBFF	Obstacle-Based Barrier Force Field
OSG	OpenSceneGraph
PRF	Parametric Risk Field
PRF-CRF	PRF Contour Risk Field
PRF-ICF	PRF Inlets Contour Field
SafAS	Safety Augmentation System
SCRF	Static Circular Risk Field
SELRF	Speed-Based Ellipse Risk Field
SSD	Solution Space Diagram
UAV	Unmanned Aerial Vehicle

Contents

List of Figures

List of Tables

Part I

Scientific Paper

Increasing Acceptance of Tactile Feedback in UAV Teleoperations by Visualizing Force Fields

V. Ho*, C. Borst†, M. M. van Paassen‡ and M. Mulder∀

***Abstract*—Due to the increasing complexity of controlling Unmanned Aerial Vehicles (UAVs), researchers have been trying to let automation take part of the UAV control in order to eliminate human error and reduce the workload of the operator. Such a system has been developed for UAV teleoperators which incorporates haptic feedback on the control stick based on a Collision Avoidance System (CAS). When nearing obstacles, the operator gets redirected by the haptic feedback and so avoiding a possible collision. However from previous and similar studies it was stated that haptic interfaces have a low user acceptance due to the limited knowledge and insight of the pilots on the automation. To improve the acceptance of the haptic feedback system this research adds additional visualizations to an existing interface. In order to evaluate these newly designed visuals, a human-in-the-loop experiment was performed. Results show that there were no significant differences between the different configurations, however, acceptance questionnaires filled in by the participants revealed that they preferred operating an UAV with additional visualizations. This means that raising the acceptance of the haptic interface was accomplished without deterioration of the operators safety, performance and workload.**

Keywords - Unmanned Aerial Vehicles (UAV), haptic interface, haptic feedback, tele-operations, collision avoidance, artificial force field, human-machine interaction, acceptance tactile feedback, haptic shared control.

I. Introduction

OPERATING UAVs can be a challenging task whether flying a small toy quad-copter or a military grade drone. For most flights they are still controlled by a pilot through remote control. In cases where the UAV flies outside the line of sight, the drone is controlled by teleoperation. However, places with low visibility due to the lack of light or because of obstructions like smoke pose a real threat to teleoperation since the cameras and electro-optical sensors cannot provide quality images [1]. Navigating through environments like these can be very challenging for the operator and may result in a crash. Human factor issues are present in 21% to 67% of UAV accidents [2]. The teleoperator lacks multiple-sensory information of the surrounding environment (e.g., vehicle motion, vibrations, environment/vehicle sound and outside view) compared to pilots flying in a manned aircraft [3]. The information is usually provided by visual displays from on-board cameras and sensors which have limited resolution and Field of View (FOV) [4,5].

In order to compensate for the lack of direct sensory input from the environment, a haptic interface has been developed for collision avoidance [6]. This method consist of a haptic feedback system and Collision Avoidance System CAS. The CAS uses an Artificial Force Field (AFF) to map environmental constraints to steering commands for avoiding collisions with objects [7]. Combining this with a haptic feedback system which provides information through the sense of force on the control device, results in a shared control system between human and automation. However, research states that shared control systems are still not optimal [8]. That is also the case for this haptic interface. Although most reports are positive, pilot/operator acceptance is sometimes a problem [8,9]. This can be due to the lack of information of why and how the haptic system works [6,10].

A similar case of an acceptance problem was investigated by Seppelt [11] on Adaptive Cruise Control (ACC). It was shown that the driving safety was compromised if the drivers did not understand how the ACC functioned. By applying Ecological Interface Design (EID) to create a visualization of the ACC behavior, they intended to promote appropriate reliance and support effective transitions between manual control and ACC. Using this knowledge of relevant topics and other past research [10,12] an additional visualization is suggested to challenge this problem of low acceptance of haptic feedback for UAV teleoperations. By combining the already existing haptic interface with a new display, an experimental haptic interface is created. The main goal of this research is therefore to design and evaluate these new visualizations in terms of acceptance, performance and safety.

In Section II the existing haptic interface will be explained. The design and development of the visualization is described in Section III. A description of the human-in-the-loop experiment that was performed is given in Section IV. Section V gives the results that followed from this experiment. A discussion of the results and recommendations for future research is given in Section VI. This research is concluded in Section VII.

II. Haptic Collision Avoidance System

The aim of a haptic collision avoidance system (HCAS) is to increase the safety and performance of UAV teleoperations while trying to improve teleoperator situation awareness (SA) and workload. As mentioned in the introduction, Boschloo and Lam have developed a HCAS that provided a satisfiable results [6,13]. This section will elaborate the workings of this system. The first subsection gives an overview of the overall architecture of the HCAS while the second subsection gives more details about the artificial force field that is generated by the system. Finally, in the third subsection previous research on the haptic interface is elaborated.

A. System Architecture

To help the teleoperator piloting the UAV, the haptic interface informs the operator if a certain control input will lead to a higher risk of an obstacle collision. To realize this feature, the surrounding environment of the UAV is identified by using an obstacle detection system. The detection is done by a Laser Imaging Detection And Ranging (LIDAR) sensor. This system measures the distance from UAV to object by analyzing the reflected light by the laser beam mounted below the UAV. The laser scans the environment in two dimensions, returning distance measurements at specific angle intervals. With this

*MSc Student, Control and Simulation Division, Faculty of Aerospace Engineering, Delft University of Technology; v.ho@student.tudelft.nl

†Assistant Professor, Control and Simulation Division, Faculty of Aerospace Engineering, Delft University of Technology; c.borst@tudelft.nl

‡Associate Professor, Control and Simulation Division, Faculty of Aerospace Engineering, Delft University of Technology; m.m.vanpaassen@tudelft.nl

∀Professor, Control and Simulation Division, Faculty of Aerospace Engineering, Delft University of Technology; m.mulder@tudelft.nl

All authors can be reached at: P.O. Box 5058, 2600GB Delft, The Netherlands

mapping, which replicates the visual control task of the pilot, the so called AFF computes the risk of collision. The risk is then converted to a certain haptic moment which acts on the control stick as haptic feedback to warn the pilot of a potential collision with an object. A schematic representation of the haptic interface is shown in Figure 1. From this figure the upper blocks represent the control loop if there was no haptic feedback. With the addition of the lower blocks, the haptic system is integrated.

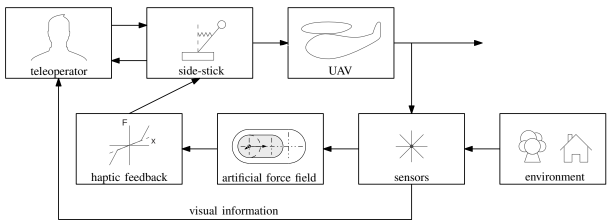

Figure 1: Schematic representation of haptic interface for UAV teleoperations

B. Artificial Force Field

The design of the haptic interface of Lam [6] starts with defining an AFF which is one of the two main components of the haptic system as discussed in the previous section. This AFF, which moves with the UAV, also referred as a "potential field", is used to map environmental constraints to imaginary forces acting on a vehicle. An obstacle generates a repulsive force by taking the gradient of the potential field. These repulsive forces can be used for CAS using haptic feedback. The CAS and thus AFF work from a two dimensional top-down view.

The current state-of-the-art AFF, the Parametric Risk Field (PRF), designed by Boschloo et al. is used specifically for UAV teleoperations [13]. This AFF was thoroughly analyzed and evaluated by Lam, which research revealed positive results regarding it use as HCAS. The parameters and variables which define the size and shape of the PRF can be seen in Figure 2.

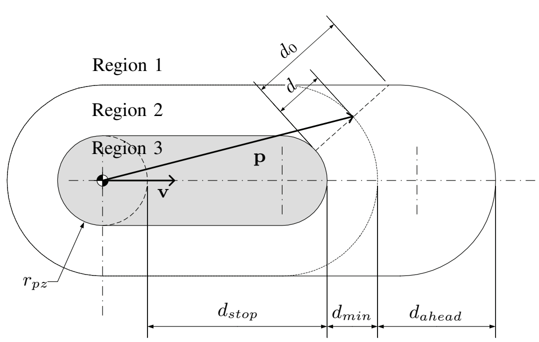

Figure 2: Parameter and variable definitions for Parametric Risk Field [6].

Around the UAV is the "protected zone" r_{pz}, any obstacles in this area means a collision. The risk field is extended by d_{stop} and d_{ahead} when the UAV is moving and is simply defined by two equations.

$$d_{stop} = \frac{|\mathbf{v}|^2}{2a_{max}} \tag{1}$$

$$d_{ahead} = |\mathbf{v}|t_{ahead} \tag{2}$$

The shape is proportional to the UAV velocity $\mathbf{v}$ and to its maximum deceleration a_{max}. If the UAV has zero velocity, the PRF becomes a small circular region around the vehicle as seen in Figure 3a. When moving, the PRF extends in the direction of the flight path as seen in Figure 3b.

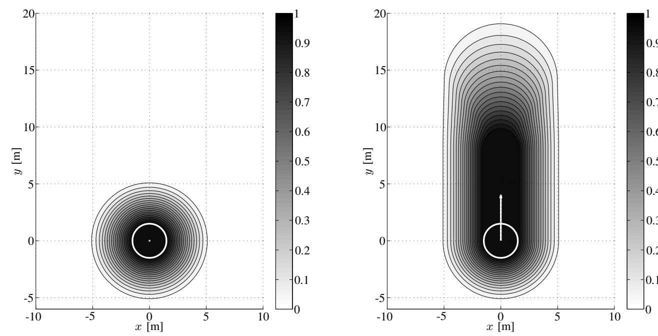

(a) $v = 0m/s$ (b) $v = 4m/s$

Figure 3: Two-dimensional contour plot of the Parametric Risk Field for two different UAV velocities. The colorbar indicates the risk of collision

The time parameter, t_{ahead}, can be changed in order to let the operator have more or less time to react to obstacles in the direction of motion. In total the PRF geometry is defined by these parameters: r_{pz}, t_{ahead}, a_{max} and d_{min}. The values of the parameters in this research have been optimized by Lam [6] and can be seen in Table I.

Table I: Optimized parameters for the geometry of the Parametric Risk Field

Parameter	Value	Description
r_{pz}	1.5	Protection zone radius $[m]$
t_{ahead}	2	Available reaction time $[s]$
a_{max}	1	Maximum UAV deceleration $[m/s^2]$
d_{min}	1.5	Distance between region 1 and region 3 $[m]$

An AFF computes the risk of collision based on the relative distance between the UAV and the obstacle $\mathbf{p}$. The risk, which scales from 0 to 1 with 0 representing a minimum risk and 1 the maximum risk, depends on the region in which the obstacle is located and the instantaneous UAV velocity $\mathbf{v}$. So the potential function for calculation the risk is as follows:

$$P(\mathbf{p},\mathbf{v}) = \begin{cases} 0 & \text{if } \mathbf{p} \text{ in Region 1,} \\ cos(\frac{d}{d_0}\frac{\pi}{2} + \frac{\pi}{2}) + 1 & \text{if } \mathbf{p} \text{ in Region 2,} \\ 1 & \text{if } \mathbf{p} \text{ in Region 3.} \end{cases} \tag{3}$$

The cosine function which computes the risk in region 2 enables a smooth transition in risk values from region 3 to region 1. To evaluate this function the distances d and d_0 can be taken from figure 2.

With the potential function defined and the risk field known, the final avoidance force vector can be obtained. This vector is equivalent to the force feedback that the operator experiences. There are different strategies and methods to calculated this vector, but for this research the method preferred by Lam will be used [6].

The final avoidance force vector, or shortened as final avoidance vector (FAV), is obtained by taking the risk values generated by the PRF from the obstacles. Obstacles are detected with an angular resolution of 3 degrees by a discrete sensor. The risk values on the obstacle surface have a corresponding risk vector pointing towards the center of the UAV. These individual risk vectors are then used to calculate the final risk vector before transforming it to a force vector acting on the UAV. The sum of the largest positive and negative risk vector in both x and y direction equals the FAV limited to the maximum risk 1. Equation 4 shows a clarification.

$$\mathbf{FAV} = \begin{bmatrix} maxrisk_X + minrisk_X \\ maxrisk_Y + minrisk_Y \end{bmatrix} \qquad (4)$$

In Figure 4 the risk vectors can be seen from the obstacles with the FAV represented as a colored arrow in the center of the UAV pointing away from the obstacles.

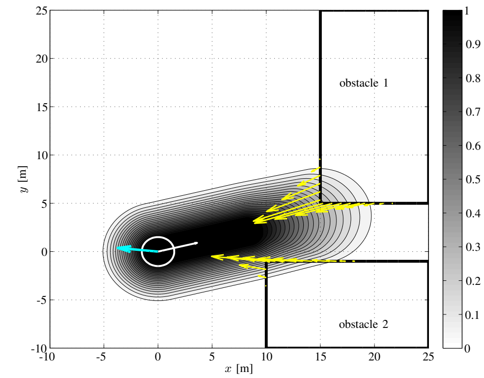

Figure 4: Risk vectors (from the obstacles) and final avoidance vector (from the center of the UAV) in a two obstacle scenario

C. Previous Experimental Research

Extensive research on the haptic interface has been done by Lam in multiple human-in-the-loop experiments [6]. Subjects, the tele-operators, were asked to fly a simulated UAV through an obstacle course. Different AFFs and haptic feedback settings were tested to see how they would affect the pilots performance. In these experiments it was found that enabling haptic feedback did indeed reduce the number of collisions and thus increasing the safety of teleoperations compared to having only manual control. Furthermore, a higher average UAV velocity was found meaning that the flight performance also increased. However, the experiments also revealed that the overall subjective workload was higher when the haptic feedback was enabled. This was caused by the increase of physical workload and frustration due the different feedback configurations [6]. Subjects explained that at some moments the haptic feedback was ‘too strong’ or ‘too unpredictable’. The haptic interface did improve the pilots performance, but it had a mixed user acceptance rating. This was also the case for similar research conducted by Kolsteeg and Sunil [14,15] on the same interface. To improve the pilot’s acceptance rating and continuing to enhance this interface, a new visualization is introduced in the following section.

III. Haptic Feedback Visualization Designs

Teleoperators using the haptic interface fly a simulated UAV using two displays. A simulated on-board camera view is projected on a screen in front of the operator, Figure 5a, while a separate navigation display, also in front of the user, presents a top-down view of the nearby environment as seen in Figure 5b.

As mentioned in the introduction, state-of-the-art solutions use extra visualizations for the user to improve the acceptance of automation. This way the operator knows when and why the ‘unknown’ automation is activated. The proposed solution for the haptic interface for UAV teleoperations is therefore also an extra visualization. The process of designing and selecting the appropriate additional visualization is done in this section.

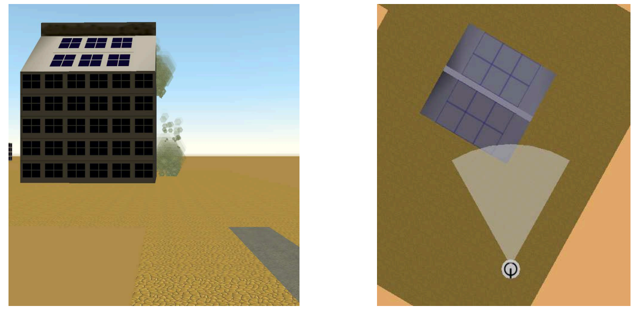

(a) 3-dimensional on-board camera display

(b) 2-dimensional navigation display

Figure 5: On-board camera and navigation display

The first question that is raised, is where the visualization should be situated. Two options were possible: on the on-board camera view or on the top-down view. Following the results of the research of Borst [10] which also presented additional visual information of haptic feedback on either the Navigation Display (ND) and Primary Flight Display (PFD), it was found that information shown on the flight display induced clutter and was redundant. Similarly but not directly related with haptic feedback, shared control/automation systems in modern cars (automated parking systems, adaptive cruise control and lane keeping systems) also display their current situations on a separate utility screen [11,16–18]. Therefore it was chosen to develop a visualization on the navigation display for a familiar user experience.

The second and most important question is what visualization may be optimal for UAV teleoperations. This is a rather difficult question to answer since for every scenario and person the preference of flight display will differ. Therefore, a solution that satisfies the need for visualization in most situations and provides accurate representation of the haptic feedback, given by the PRF, will be considered.

A. PRF Contour Risk Field

To provide a visualization that corresponds with the haptic feedback, the most logical option would be to reproduce the PRF directly on the display. This gives the operator direct visual information on how the PRF behaves according to the UAV motions. It, however, provides the user excessive information like layers of different risk, risk vectors and FAV. The visualization expects the teleoperator to have full knowledge of how the PRF and its calculations work while cluttering the navigation screen. This would result in a high mental workload and distraction for the pilot flying the UAV. Therefore a slimmed-down version of the PRF visualization is made, called PRF Contour Risk Field (PRF-CRF). A schematic overview of this visualization can be seen in Figure 6a.

This visualization displays the geometry of the PRF, (1) in Figure 6a, around the UAV (5) like the algorithm, but it leaves out all the information inside the outer contour. The outer contour is the boundary between region 1 and region 2 as seen in Figure 2. Furthermore, the risk vectors are reduced to simple colored dots (4) which have a color code that show how much risk they represent. White means low risk and barely feel-able haptic feedback, yellow means medium risk and noticeable feedback and red means maximum risk and gives the maximum amount of feedback. These two changes to the visualization are expected to allow the user to quickly understand that when the outer contour crosses an obstacle (2), colored dots will appear which pose a certain risk with associated haptic feedback. The last element of this design is the FAV. It is a simple vector line (6) attached to the center of the UAV and which grows in length and direction according to the magnitude and direction of the haptic feedback force. The final result of this visualization can be seen in Figure 6b.

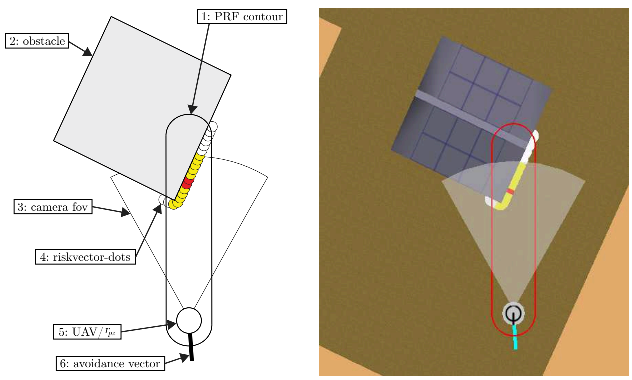

(a) PRF-CRF description (b) PRF-CRF during flight

Figure 6: PRF Contour Risk Field in a one obstacle scenario

B. Static Circular Risk Field

To test whether the geometry of the visualization, thus directly relateable to the PRF, matters, a second design option is considered. This alternative would provide the user with a different visualization which still uses the PRF algorithm but does not correspond visually with the algorithm. With this visualization it can be tested if a large (PRF-CRF) or little resemblance between visuals and algorithm would provide a difference in terms of acceptance, performance and safety of UAV teleoperations. The Static Circular Risk Field (SCRF) is as the name says a static circle, (5) in Figure 7a, around the UAV (4). The idea of using a static circle comes from a research concerning airborne separation [19] which uses a static half-circle on the navigation display to aid pilots in finding conflict resolutions. In comparison with the PRF-CRF the outer contour does not alter according to the geometry of PRF. The amount of clutter should be reduced by this since less displacement of visuals is visible. The radius of the circle is pre-defined to accommodate the test scenarios. Instead of feeding the user the exact location and size of the risk vectors like in the PRF and PRF-CRF, only the angular data and size are shown. This is done by displaying the location and size of the risk vectors as colored lines (3) within the static circle. A risk vector at a certain location has a known angle with respect to the UAV, so using the same color coding as the PRF-CRF, a white/yellow/red line is shown in the direction of this particular risk vector. By repeating this step for all risk vectors, a directional 360 degrees risk map can seen within the circle. The risk map should be easier to understand for the pilot compared to the PRF-CRF since they should just avoid flying in the direction of the risks. The last component of the PRF, the FAV, is not shown in the SCRF and is replaced by a ‘highest risk’ line (red line of element (3)). It tells the user in which direction the current highest risk is present. This was added to avoid confusion when a separate angular risk vector would overlap the FAV. The final result of this visualization can be seen in Figure 7b while a detailed schematic sketch can be seen in Figure 8.

There are several arguments for designing the SCRF as the second configuration. The primary reason is that it does not have velocity dependent moving element like the PRF-CRF. While it might be useful in some cases, it can clutter the ND and hinder the flight performance of the pilot. Especially when accelerating and decelerating quickly the PRF contour might distract too much and cause confusing about

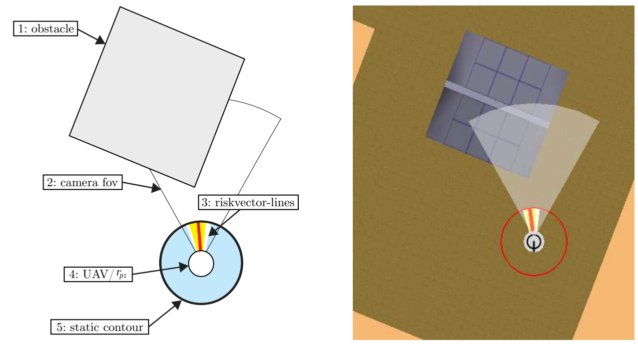

(a) SCRF description (b) SCRF during flight

Figure 7: Static Circular Risk Field in a one obstacle scenario

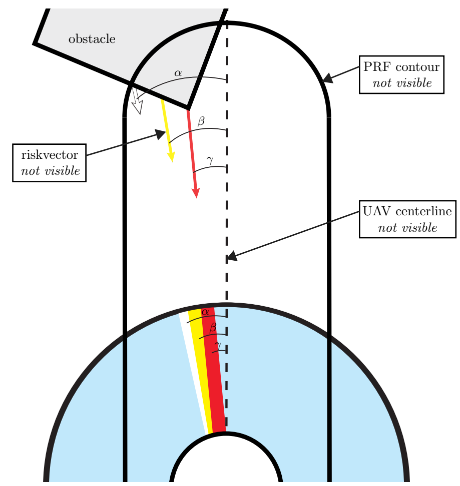

Figure 8: Static Circular Risk Field detailed overview on workings

possible collisions because the PRF boundary overlaps the obstacle as seen Figure 6b. The SCRF does not have this problem with its static circle. Another reason for this design is familiarity from video games. In many games where the player operates an air/space-craft, the user is also presented a circular mini-map [20,21]. This static circular map usually displays lines or arrows in the direction of incoming obstacles (enemy-fire or debris). Based on these user interface designs, the SCRF might feel familiar and intuitive for the teleoperator. One last reason for the SCRF is the simplicity of the design. It uses very few drawing elements and thus reduces the processing power needed of the hardware in comparison with the PRF-CRF.

The main differences and elements of the two visual designs are presented in Table II.

Table II: Elements of PRF-CRF and SCRF

Element	**PRF-CRF**	**SCRF**
PRF Algorithm	Only outer contour visible	*Not visible*
Risk Vectors	On obstacle, by colored dots	On risk map around UAV, by colored risk lines
FAV	Blue vector line attached on UAV	*Not visible*
Highest Risk	*Not visible*	Red vector line on the risk map

IV. Human-in-the-loop Experiment

A human-in-the-loop experiment was conducted to investigate the haptic interface with the two new visualizations. The experiment should determine how extra visualizations affect the operator with respect to the previous haptic interface. The setup of this experiment is very similar to the experiments performed by Lam [6]. One main difference is that no haptic configurations were altered during the experiment. All participants flew with the same haptic configuration and only the visualizations were changed.

A. Participants

In total there were twelve participants, all male and right-handed with an average age of 25.08 years (σ =0.86 years), who participated in the experiment. The participants consent was obtained before starting the experiment and received no monetary compensation.

B. Apparatus

This experiment was conducted in a fixed-base flight simulator of the Human-Machine Interaction lab (HMI-Lab) at the faculty of the Aerospace Engineering of TU Delft. The simulator can be seen in Figure 9. The participants were seated in an aircraft chair (1) with an electro-hydraulic side-stick and arm rest (2) mounted on the right side. The visualization of the experiment is provided by two displays. An 18-inch LCD screen with a resolution of $1280x1024$ pixels at $60Hz$ in front of the participant is used as navigation display (3). Furthermore an on-board camera view (4) is projected on a white wall by a 1080p projector approximately 3 m in front of the participant with a resolution of $1344x756$ pixels at $60Hz$. The UAV camera view has a FOV of 60 degrees horizontally and 45 degrees vertically and is fixed to the longitudinal axis of the UAV.

C. Instructions

The main task of the participants was to fly an UAV from waypoint to waypoint (represented as smoke plumes) in an obstacle filled urban environment containing multiple buildings. Participants were given the instruction to fly through the obstacle course, while avoiding collisions (highest priority), as closely as possible through the waypoints (second priority) and as fast as possible (lowest priority). When a collision did occur, a time penalty was given in which the experiment was paused for 10 seconds and a loud beeping sound was simultaneously played. After the penalty, the UAV position resets to a specific starting position of the course and the experiment is resumed.

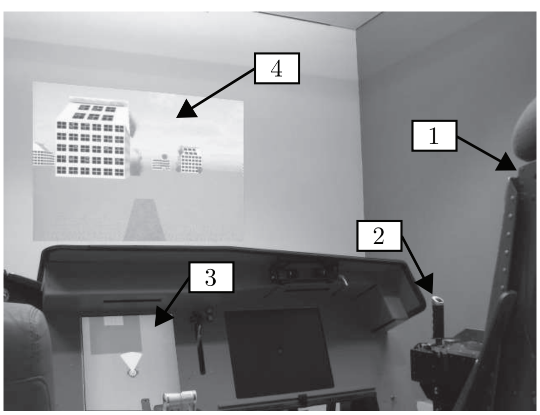

Figure 9: Experiment room setup

D. UAV Model

The experiment used a control-augmented UAV helicopter model with easy controllability which is the same as the one used by Lam [6]. A longitudinal stick deflection represents a velocity command along the x-direction, whereas a lateral deflection results in a turn rate with a maximum of $0.32rad/s$. The model has a maximum velocity of $5m/s$, a maximum acceleration of $1m/s^2$ and a maximum turn acceleration of $2rad/s^2$. The altitude of the UAV is kept constant by control augmentation.

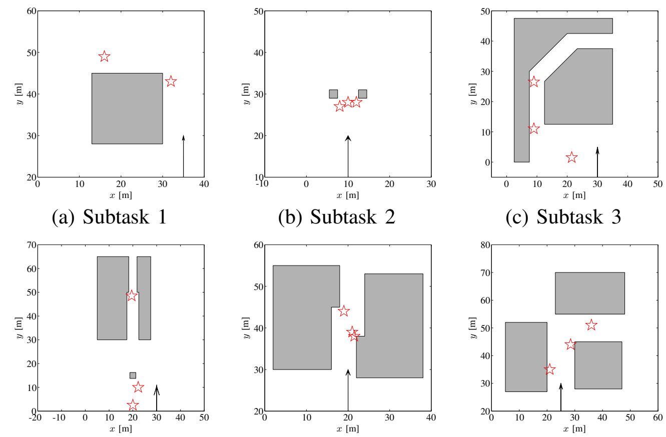

(a) Subtask 1 (b) Subtask 2 (c) Subtask 3

(d) Subtask 4 (e) Subtask 5 (f) Subtask 6

Figure 10: Six different subtasks that are present in all trajectories. The stars indicate the waypoints that are displayed as smoke plumes in the camera view. The arrows indicate the flight direction which should be taken by the participant.

E. Independent Variables

There were two independent variable for this experiment: the visualization configuration for the navigation display and the subtasks within the trajectory which the participants had to fly. The three different configurations that were tested by all participants are as follows:

- NV: No Visualization (NV), the baseline of this experiment.
- PRF: Parametric Risk Field (PRF), design option (PRF-CRF) is used as visualization in this configuration.
- SCRF: Static Circular Risk Field (SCRF), design option (SCRF) is used as visualization in this configuration.

The six subtasks, which can be seen in Figure 10, are separate trajectory blocks in which the pilot has to perform a different maneuver. All participants had to fly three different trajectories in which all six subtasks were present.

The haptic configuration was kept constant for all participants as mentioned before. Multiple haptics settings were defined and analyzed by Sunil [15]. It was concluded that the "Relax Task (RT)" tuning setting was most suitable for UAV teleoperation, hence this setting was used for the experiment.

F. Dependent Measures

There are in total five different dependent measures groups that are measured. An overview of all the measures is giving in Table III.
Questionnaires were used to measure the subjective workload and operators acceptance. The workload was measured using the NASA Task Load Index (NASA-TLX) questionnaire [22]. Operator acceptance measured using two forms, one was the Controller Acceptance Rating Scale (CARS) [23] and the second a questionnaire with various questions about acceptance and preference.

G. Trajectories

For this experiment the trajectories which are flown by the participants are based on those used by Kolsteeg [14]. One trajectory

Table III: Dependent measures

Measure	Metric	Description
Safety	N_{col}	Number of collisions [-]
	$\bar{R}$	Mean risk magnitude [-]
	D_{min}	Min. distance obstacles and UAV $[m]$
Performance	T_{tot}	Total elapsed time $[s]$
	D_{wp}	Min. distance waypoint and UAV $[m]$
	$\bar{\mathbf{v}}$	Mean velocity $[m/s]$
Control Activity	SRR	Steering Reversal Rate $[-]$
	$\sigma_{\dot{\delta}_{st}}$	Standard deviation stick rate $[rad/s]$
	$\bar{M}_{NMS}$	Mean neuromuscular moment $[Nm]$
Haptic Activity	M_{Hap}	Mean haptic moment $[Nm]$
Subjective	NASA TLX	Subj. workload assessment [-]
	CARS	Subj. acceptance assessment [-]
	AQ	Subj. acceptance questionnaire [-]

consists of six different subtasks which are presented in a randomized order. Each subtask required a specific maneuver to let the pilot devise different control strategies. In each of these subtasks waypoints were displayed as smoke plumes to both measure the flight performance and reduce the visibility around the obstacles. These smoke plumes were only visible on the on-board camera display.

Three different trajectories, as seen in Table IV, have the same six subtasks, only in a different order. The order of these subtasks remained the same for all participants. An example of such a trajectory is seen in Figure 11. The number of the trajectories were not enough to test every order of subtasks, so the trajectories were as contrasting as possible to reduce order effects.

Table IV: Subtask order for three different trajectories

Trajectory	Subtask order
Traj-1	1-2-3-4-6-5
Traj-2	3-1-4-5-6-2
Traj-3	4-1-5-3-2-6

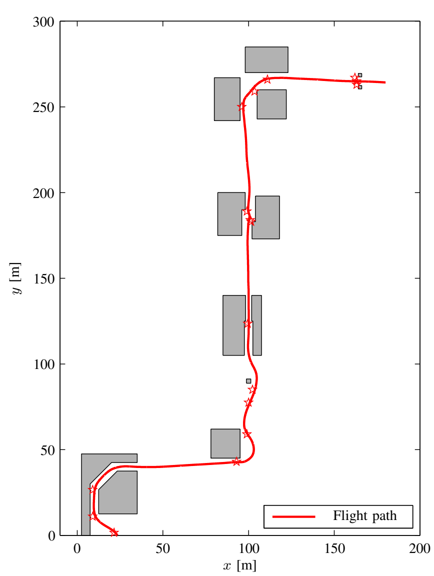

Figure 11: A single flight trajectory (Traj-2)

H. Experiment Procedure

Before the actual experiment, each participant received a short briefing. The participant got the opportunity to familiarize with the simulation environment and the three different visualization configurations. After an initial set of training runs and confirming that the training was sufficient by the participant, the measurement runs were started. For each configuration three different trajectories were run, so that means that each participant did a total of nine runs. All three conditions were randomized using the 'Latin Square' method. This was done to minimize the effect of unwanted variability of the dependent variables. Participants were not informed which condition they were performing and after each condition they were requested to fill out a NASA-TLX and CARS. Between each condition a small break was held to avoid fatigue. After the nine measurement runs a final questionnaire had to be answered. The total duration of the human-in-the-loop experiment including briefing and training was two hours.

I. Hypotheses

The following hypotheses are defined for the human-in-the-loop experiment and are based on previous research on this topic:

- *The proposed extra visualizations improve the safety of UAV teleoperators compared to the normal interface.* The visualizations show why the haptic feedback is activated and give the pilot a visual confirmation of a possible collision. The user can steer away sooner from the obstacles to avoid collision.
- *The proposed extra visualizations increase the performance of UAV teleoperators compared to the normal interface.* By paying attention to the visualizations, the operators can fly closer to objectives without triggering the CAS and fly at a higher velocity. This allows the teleoperator to fly a more efficient route and decrease the total elapsed time.
- *The proposed extra visualizations change the control strategies of UAV teleoperators compared to the normal interface.* With the early warning signs of the visualizations, the operator can decide to take an alternative flight path to avoid unnecessary risk or activation of the haptic feedback.
- *The proposed extra visualizations decrease the workload of UAV teleoperators compared to the normal interface.* When flying past obstacles, the visualizations indirectly show areas where less haptic feedback can be expected thus reducing the physical and possibly mental workload.
- *The proposed extra visualizations increase the acceptance of the haptic interface for UAV teleoperators compared to the normal interface.* Pilots can use the visualizations to 'predict' when the haptic feedback will start to kick in and therefore reduce the frustration with unpredictable activations. It also tells the user why the haptic feedback is giving a strong counter force because close proximity obstacles. This provides the pilot the confirmation to work with the haptic system instead of against.

V. Results

The main results of the experiment will be given in this section. The data analysis was done using full-factorial repeated-measures Analysis of Variance (ANOVA) with a significance level of $\alpha = 0.05$. Any significant result were further evaluated with post-hoc tests, pairwise Bonferroni and Greenhouse-Geisser (GG) corrections were applied to the data. Measures with ordinal variables were tested with a non-parametric Friedman test with Wilcoxon matched signed rank for post-hoc analysis or a Kruskal-Wallis test with Mann-Whitney post-hoc. Runs where a collision occurred were not taken into account in the analysis except for the collision measure. For each participant the dependent variables of multiple runs of the same subtask were averaged. The graphs for each variable are visualized in both configuration specific (CONS) and subtask specific (SUBS) to show if there is a relation between subtask and configuration. All significant results in the following subsections are related to the SUBS output. No statistically significant effect was found in the overall configuration results displayed in the Figures 12a–14a and 16a–26a.

A. Safety

The number of collisions, N_{col}, in Figure 12 show that more collisions occur with the visualization on. This is especially noticeable in subtask 4. Subtask 4 was reported by the participants as the most difficult one because of the small corridor in which they had to pass through. Three pilots using the SCRF collided twice in this particular subtask. No statistically significant difference was found between the configurations, in contrast, between subtasks there was a high significant effect (SUBS: $\chi^2(5) = 23.09, p \leq 0.01$). No interactions between CONS and SUBS were observed. The total number of collisions, 108 total runs and 26 collisions, is comparable with previous research of Lam (40 runs, 8 collisions) and Sunil (180 runs, 24 collisions) [14,15]. It must be noted that subtasks 3 and 4 of their research have been replaced by the current significantly different subtasks.

The mean risk magnitude, $\bar{R}$, is shown in Figure 13. The risk magnitude is the risk of collision calculated by the PRF. From the figure it can be seen that for all configurations there is almost no difference in risk. So the only statistically significant effect can be found between subtasks in the SUBS result (SUBS: $F_{1.86,20.44} = 135.19, p \leq 0.01$, GG). This can be explained by the subtask geometry and the placement of waypoints. For subtasks 3 and 4 the operator has to fly through a narrow corridor creating a higher risk because of the close proximity to both walls. In subtasks 5 and 6 the waypoints are placed close to the walls, forcing the operator to fly closer and thus creating more risk. With visualizations on, the results show a slightly lower median in comparison with no visualization for the more difficult subtasks. No interactions between CONS and SUBS were observed.

The last safety measure, the minimum distance to obstacles from the UAV, D_{min}, is seen in Figure 14. Again, no considerable differences can be found here except in subtask 1, 5 and 6. Between the participants there is a large spread in minimum distance for these subtasks. This can be due the space available between obstacles giving the operator more freedom to maneuver and fly a different strategy. In Figure 15 the flight trajectories of the pilots can be seen. It is noticeable that for all configurations the paths are very similar and that the larger spread in results can be seen in the mentioned subtasks. A significant effect was found for the SUBS results. Between the configurations (CONS: $F_{2,22} = 5.91, p \leq 0.01$) and subtasks (SUBS: $F_{1.98,21.79} = 73.56, p \leq 0.01$, GG). No interactions between CONS and SUBS were observed.

These results show that the visualizations do not give significant differences regarding the safety. The first hypothesis is therefore rejected.

B. Performance

The total elapsed time, T_{tot}, is plotted in Figure 16. No significant differences can be identified between the configurations. The short and easy subtask 2 resulted in a significant difference (SUBS: $F_{1.88,20.60} = 245.00, p \leq 0.01$, GG). No interactions between CONS and SUBS were observed.

The next measure is the minimum distance between the waypoints and the UAV, D_{wp}. The results in Figure 17 show that there are

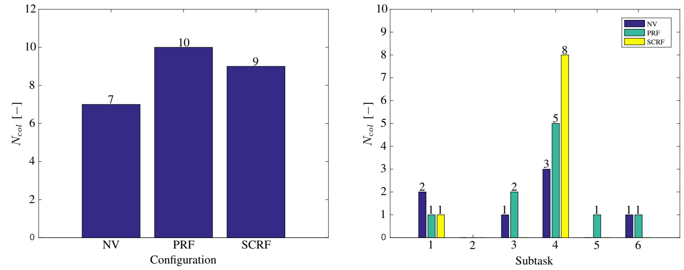

(a) Configuration overall (b) Subtask specific

Figure 12: Number of collisions bar charts for both configuration and subtask separately

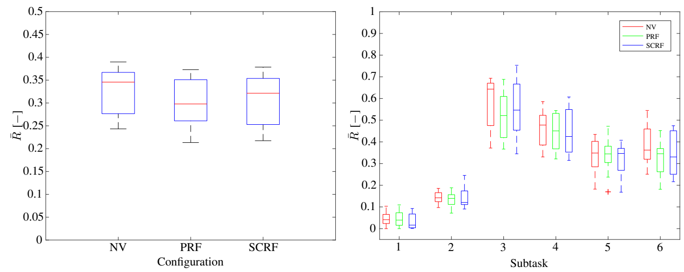

(a) Configuration overall (b) Subtask specific

Figure 13: Mean risk box plots for both configuration and subtask separately

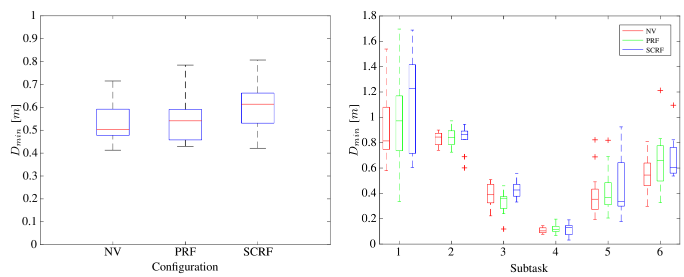

(a) Configuration overall (b) Subtask specific

Figure 14: Minimum distance from obstacles box plots for both configuration and subtask separately

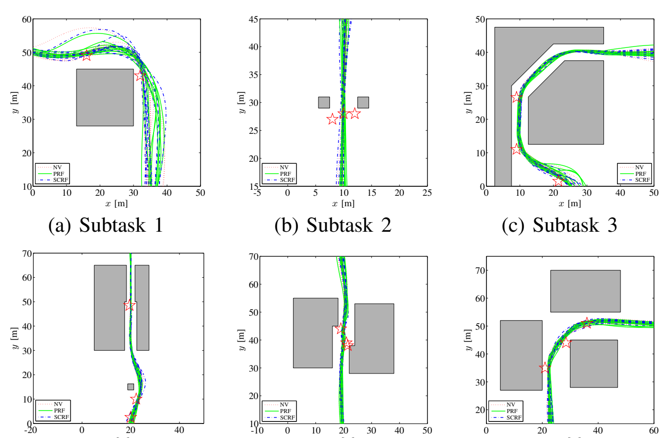

(a) Subtask 1 (b) Subtask 2 (c) Subtask 3

(d) Subtask 4 (e) Subtask 5 (f) Subtask 6

Figure 15: Flight trajectories of participants in all subtasks for one scenario.

again no differences in the different configurations. The large spread of subtask 1 can be explained by the different flight strategies of the participants. Because the waypoint was hidden behind the obstacle when approaching the corner, many participants did not turn sharp enough to reach the waypoint on time as can be seen in Figure 15a. The distance to the waypoint is the smallest for subtask 2. The reason for this is that the operators had to fly through a gate where the waypoint was located in the center. Because of this major difference, the subtasks in the SUBS results show a significant effect (SUBS: $F_{1.11,12.18} = 24.59, p \leq 0.01$, GG). No interactions between CONS and SUBS were observed.

The last measure of the performance group, the mean velocity of the UAV, is shown in Figure 18. For all subtasks, the velocity seems to be fairly constant for all configurations. Therefore no significant effect can be found between configurations. The short and easy subtask 2 resulted in a significant difference in the SUBS results (SUBS: $F_{5,55} = 38.32, p \leq 0.01$). No interactions between CONS and SUBS were observed.

Following the results of the performance measures, it can be said that the visualizations do not increase the flight performance of the teleoperator. The second hypothesis is therefore rejected.

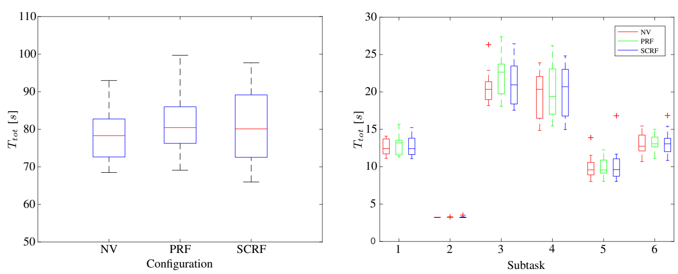

(a) Configuration overall (b) Subtask specific

Figure 16: Time elapsed box plots for both configuration and subtask separately

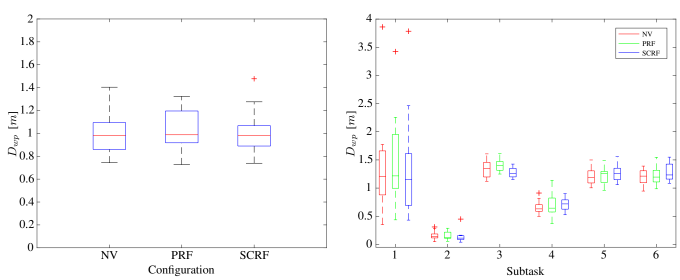

(a) Configuration overall (b) Subtask specific

Figure 17: Waypoint distance box plots for both configuration and subtask separately

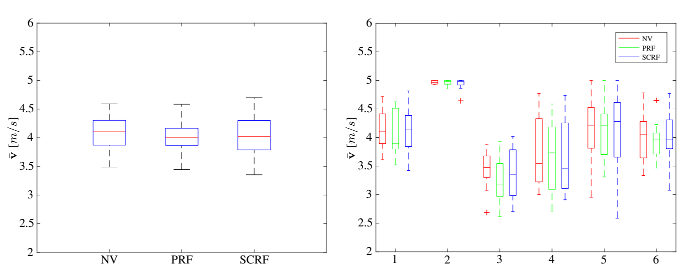

(a) Configuration overall (b) Subtask specific

Figure 18: Mean velocity box plots for both configuration and subtask separately

C. Control Activity

Figure 19 shows the plots of the Steering Reversal Rate (SRR) in longitudinal direction, SRR_X. The CONS only graph displays a much wider spread of data points with the visualization on. This effect is slightly less, but still visible on the SUBS plot. It however does not provide a statistically significant effect. Since almost no turns were needed in subtask 2, it resulted in a significant effect for longitudinal (SUBS: $F_{1.77,19.42} = 132.42, p \leq 0.01$, GG) and lateral (SUBS: $F_{1.66,18.21} = 194.48, p \leq 0.01$, GG) SRR. In lateral direction the SRR_Y has even less spread, as seen in figure 20. No interactions between CONS and SUBS were observed.

The standard deviation of the side-stick deflection rate in longitudinal, $\sigma_{\dot{\delta}_{st_X}}$, and lateral, $\sigma_{\dot{\delta}_{st_Y}}$, direction are shown in Figures 21 and 22. No significant effect can be identified for both measures. The results between the different configurations were very similar. Since almost no turns were needed in subtask 2, it resulted in a significant effect for longitudinal (SUBS: $F_{5,55} = 33.23, p \leq 0.01$) and lateral (SUBS: $F_{1.92,21.06} = 25.30, p \leq 0.01$, GG) deflection rates. No interactions between CONS and SUBS were observed.

The results of the last control activity measure, the mean longitudinal and lateral neuromuscular moment, $\bar{M}_{NMS_X}$ and $\bar{M}_{NMS_Y}$, is shown in Figures 23 and 24. For both measures there is no significant difference for configurations. Because of the greatly different subtasks, there was a significant effect in the SUBS results for both longitudinal (SUBS: $F_{2.89,31.75} = 17.10, p \leq 0.01$, GG) and lateral (SUBS: $F_{1.71,18.83} = 166.02, p \leq 0.01$, GG). No interactions between CONS and SUBS were observed.

Following the results of the control activity measures, it can be said that the participants did not control their UAV any different in all configurations.

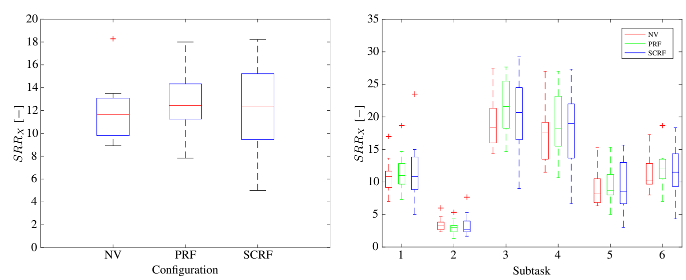

(a) Configuration overall (b) Subtask specific

Figure 19: Longitudinal steering reversal rate box plots for both configuration and subtask separately

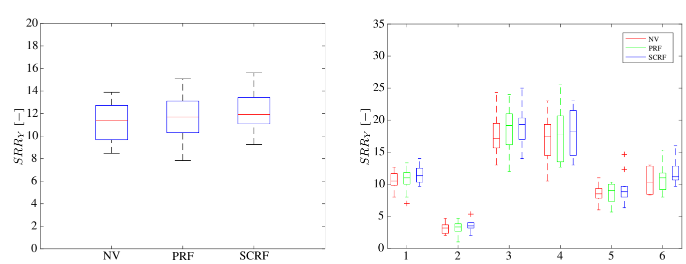

(a) Configuration overall (b) Subtask specific

Figure 20: Lateral steering reversal rate box plots for both configuration and subtask separately

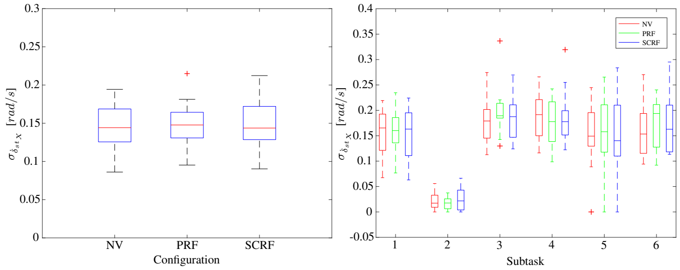

(a) Configuration overall (b) Subtask specific

Figure 21: Standard deviation longitudinal side-stick deflection rate box plots for both configuration and subtask separately

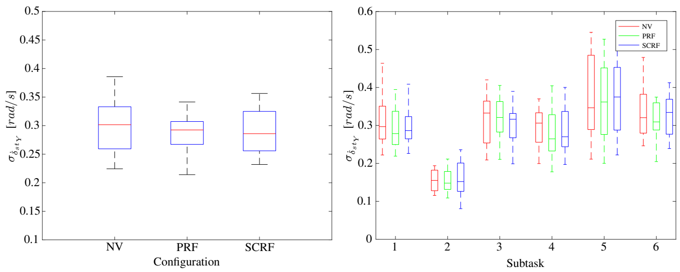

(a) Configuration overall (b) Subtask specific

Figure 22: Standard deviation lateral side-stick deflection rate box plots for both configuration and subtask separately

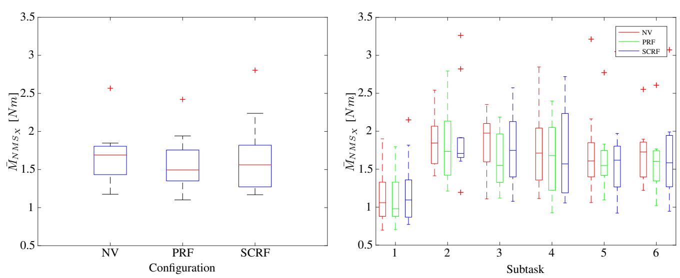

(a) Configuration overall (b) Subtask specific

Figure 23: Mean longitudinal neuromuscular moment box plots for both configuration and subtask separately

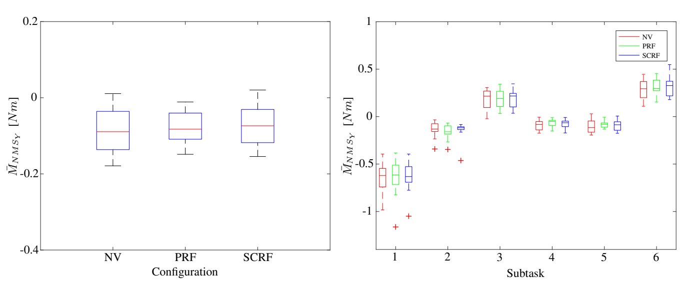

(a) Configuration overall (b) Subtask specific

Figure 24: Mean lateral neuromuscular moment box plots for both configuration and subtask separately

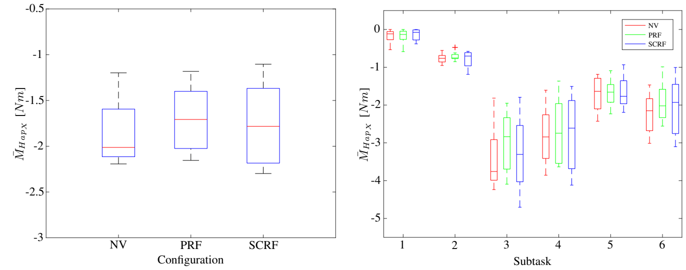

(a) Configuration overall (b) Subtask specific

Figure 25: Mean longitudinal haptic moment box plots for both configuration and subtask separately

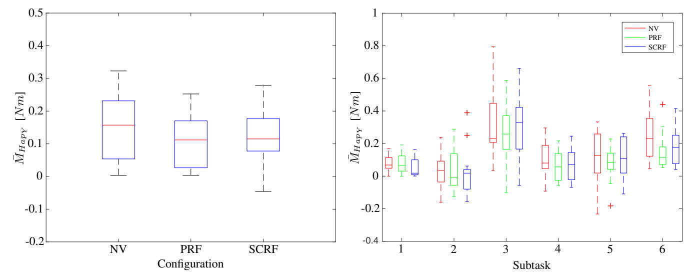

(a) Configuration overall (b) Subtask specific

Figure 26: Mean lateral haptic moment box plots for both configuration and subtask separately

D. Haptic Activity

For the haptic activity only the mean haptic moment, $\bar{M}_{Hap_X}$ and $\bar{M}_{Hap_Y}$, is measured. The results can be seen in Figures 25 and 26. No significant effect was found in the longitudinal CONS results, however in the lateral haptic moment did reveal a significant result for the different configurations (CONS: $F_{2,22} = 4.58, p \leq 0.05$). Like previous results, between subtasks there is also a significant effect visible in longitudinal (SUBS: $F_{1.49,16.42} = 91.47, p \leq 0.01$, GG) and lateral (SUBS: $F_{5,55} = 13.59, p \leq 0.01$) haptic moment. No interactions between CONS and SUBS were observed.

The longitudinal haptic moment shares a very similar result as the risk measure. The forces are also significantly higher than in the lateral direction, meaning that the main risk is directly related to the longitudinal haptic moment. In other words, the highest risk occurred in the longitudinal direction of the UAV.

E. Subjective Data

Two questionnaires were filled in after each configuration by each participants, the NASA-TLX and CARS. The results of the NASA-TLX are shown in Figure 27. A low rating means a lower workload. The overall NASA-TLX score reveals that there is almost no difference in workload for all three configurations. From the individual sources it can be seen that the ratings are fairly similar too with the exception of the SCRF frustration. Overall the visualizations have a slightly higher demand in all sources. With a Kruskal-Wallis Test no significant effect was found between configurations and the individual workload sources.

The CARS results show in Figure 29 that both PRF-CRF and SCRF have a slightly better acceptance score than the no visualization configuration. The PRF-CRF does have a better average score than the SCRF. No statistically significant effect was found.

The following results are from a questionnaire that was filled in after the experiment. They were divided in three different parts: Scaling questions, subtask questions and open questions.

For the subtask questions the participants were asked which configuration was preferred, for both overall and subtask specific. Figure 28 shows the preferred choices. So while the objective data provided no difference in safety, performance and control, the participants did prefer to fly with visualizations. The PRF-CRF is preferred by many in almost all subtasks and overall. The main reason that was given by the participants for this result was that they could use the PRF-CRF outer boundary to see when the actual haptic would trigger and thus make sharper turns. Subtask 2 was fairly easy to fly, so participants did not have a specific preference here. SCRF was preferred for subtask 4 because the PRF-CRF cluttered the screen with riskvector-dots when flying through the small corridor making it hard to see how far they were from the wall. Another mention is that occasionally a heavy framerate drop occurred when flying through the corridor of subtask 4. The lag, which lasted until the operator flew out of the corridor (a couple of seconds), also resulted in participants to prefer the SCRF.

The scaling questions are four different questions where the user had to rate their answer with a scale (1-10). The questions were about the workings of the visualization configurations. The results are displayed in Figure 30. In both the first and fourth question the participants had a clear opinion on the PRF-CRF. For the SCRF, the votes were widely spread for all four questions. Question 1 had a highly-significant effect ($\chi^2(1) = 6.879, p \leq 0.01$), post-hoc ($U = 28.5, Z = -2.62, p \leq 0.01$) while question 4 had a significant difference ($\chi^2(1) = 4.56, p \leq 0.05$), post-hoc ($U = 36, Z = -2.14, p \leq 0.05$). Additionally, the participants could give a response for this question regarding how they altered their strategy. For the PRF-CRF the general response was that they could fly closer to the walls and take more risks because the visuals showed the boundaries of the risk field. The responses for the SCRF vary much more, but it was common that the participants used the red risk vector line to either steer away from the obstacle or make tighter turns.

Finally in the open questions the participants were asked which elements of the visualizations they liked and disliked. Furthermore any additional comments to the whole haptic interface could be given. It was reported that the FAV of the PRF-CRF was not useful for most participants. The haptic feedback already provided the direction of the avoidance so visualizing the FAV was redundant. Most participants preferred the PRF-CRF when the on-board camera did not provide enough information because of the small FOV. The outer contour gave the user important information on distance between UAV and obstacle. As a final remark, users often complained about the haptic feedback itself. This was especially the case for subtasks 3 and 4 where they had to fly through a tight corridor.

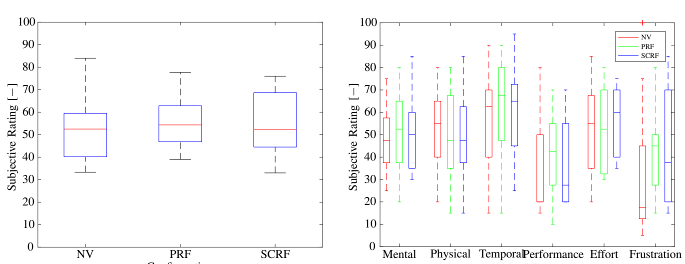

(a) Overall rating (b) Rating for specific sources

Figure 27: NASA TLX scores

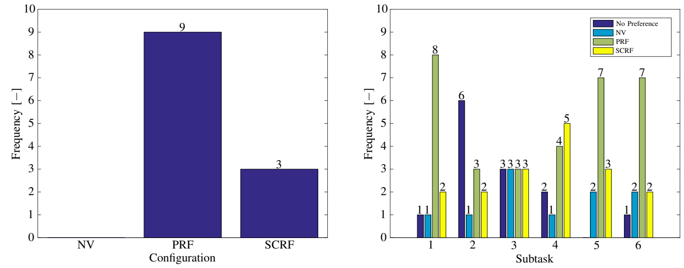

(a) Configuration overall (b) Subtask specific

Figure 28: Preferred configuration from questionnaire

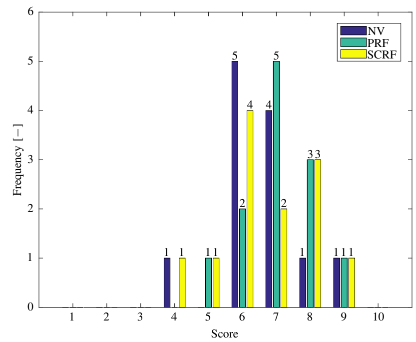

Figure 29: CARS result

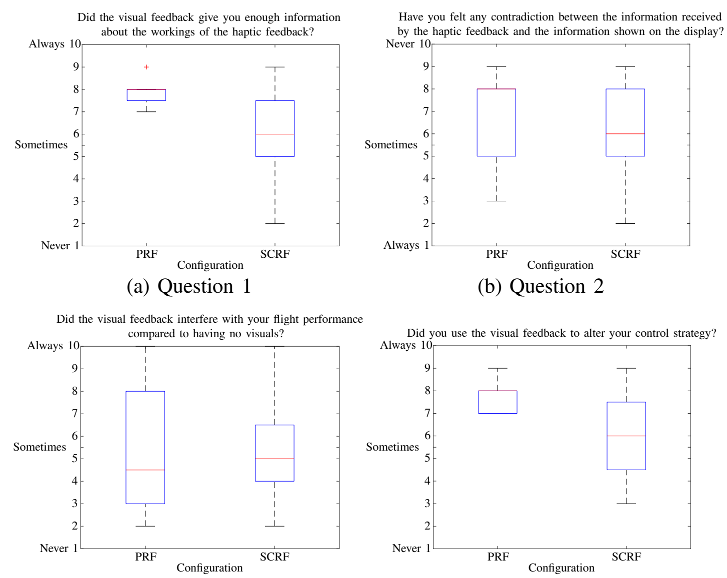

(a) Question 1 (b) Question 2

(c) Question 3 (d) Question 4

Figure 30: Scaling question box plots from questionnaire

VI. Discussion

From the introduction it was stated that by adding visualization to the haptic interface would result in an improved safety and performance of the teleoperator. Similar research on additional visualizations for haptic feedback systems yielded positive results regarding safety and flight performance. On the contrary the objective data from the human-in-the-loop experiment conducted for this research did not show any significant difference between the configurations with and without additional visualizations. A summary of the ANOVA results can be seen in Table V.

The table shows that for all metrics there was a significant effect

Table V: ANOVA Results

'**': $p \leq 0.01$, '*': $0.01 \leq p \leq 0.05$, '-': no significant effect

Measure	Metric	Significance		
		CONS	SUBS	CONS x SUBS
Safety	N_{col}	-	**	-
	$\bar{R}$	-	**	-
	D_{min}	**	**	-
Performance	T_{tot}	-	**	-
	D_{wp}	-	**	-
	$\bar{\mathbf{v}}$	-	**	-
Control Activity	SRR_X	-	**	-
	SRR_Y	-	**	-
	$\sigma_{\dot{\delta}_{st_X}}$	-	**	-
	$\sigma_{\dot{\delta}_{st_Y}}$	-	**	-
	$\bar{M}_{NMS_X}$	-	**	-
	$\bar{M}_{NMS_Y}$	-	**	-
Haptic Activity	$\bar{M}_{Hap_X}$	-	**	-
	$\bar{M}_{Hap_Y}$	*	**	-
Subjective	NASA TLX	-	n/a	n/a
	CARS	-	n/a	n/a

between the individual subtasks which gives a good impression that the subtask varied greatly. Only two metrics, minimum obstacle distance and mean lateral haptic moment, had a significant effect between the configurations. This means that by looking at the objective data, is it rather difficult to determine if the visualizations had any significant effect. With this result the hypotheses that were stated previously are mostly rejected.

To improve the safety of the UAV teleoperators, less collisions should occur with the additional visualizations enabled. When the opposite happens, one needs to analyze the results thoroughly to find any possible reason for this. From the SUBS graph it be seen that most collisions happened in subtask 4, which was a very small corridor in which the UAV has to fly through. This particular subtask received mainly negative feedback on both the haptic feedback and visuals. It was difficult for the operators to determine the spacing between the walls on the on-board camera view, so they used PRF-CRF and SCRF to navigate. In the questionnaire the participants responded that owing to the visualizations they could stay centered, however additional visualizations led to more collisions which is rather confusing. Furthermore, the PRF-CRF caused a framedrop in some occasions in subtask 4, which hindered the control of the UAV. Apparently both visualizations do not work well when the UAV is in tight-space environments (subtask 3 and 4). The participants took more risk by trusting that the visualizations gave precise information about the distance. This caused the operators to steer into the opposite wall when they thought it was almost near collision on the side.

The minimum distance from obstacle box plot shows that for tight-space environments the results do not differ that much between configurations. The interesting results come from subtasks 1, 5 and 6 where the participants had more space to maneuver. The visualizations provide the users with extra information that they can use to either to fly closer or further away from the obstacles, which can be seen in the larger spread in data points compared to the NV. Participants had their own flight strategies for open-space environments which is perfectly fine since no instructions were given to fly far-off from the obstacles, but does not give usable results for the safety hypotheses.

In the performance measure, all three metrics could not give any significant result. As seen in the flight trajectories in the individual subtasks, for all three configurations almost similar paths were taken. This means there would be almost no distinction in the performance of the operator. Having more open subtasks like subtask 1 might result in more diverse results as seen in the box plots as it gives the user more freedom in control strategy.

As mentioned in the results section, the participants did not control their UAV any different in all three configurations. This however does not coincide with the questionnaire where it was asked if the participants changed their flight strategy. So the pilots thought they were flying differently, but in reality they flew the same for all configurations. It might be that an individual participant had completely different control strategies, but the subtasks were not unique enough to show this difference, especially when you compare them with eleven other participants. The SRR box plots, Figures 19 and 20, do show that the medians of the measure with visualization enabled are slightly higher (although without significance), this can be explained by that the users made more inflight corrections because of the high risk visual warnings. This might be directly related to significant effect of the mean lateral haptic moment. Less haptic moment was generated with the visualization configurations, especially the PRF-CRF. Thus the users corrected more to avoid activating the lateral haptic feedback resulting in a lower lateral haptic moment.

The NASA-TLX revealed there was no significant difference in the workload of the teleoperator. No data can therefore be used to accept the workload hypotheses. What might be interesting to note is that the frustration has a slightly higher rating, thus worse, for the visualization configurations. Users were apparently more frustrated by the visuals, but nonetheless preferred having them on. This might be caused by not enough training and/or insufficient knowledge of the workings of the visuals. Another reason might be that, as mentioned by some participants, that the visuals had a heavy framedrop in subtask 4, causing a discrepancy between the camera/navigation display and the UAV movement. As mentioned in the results section, three participants collided twice in subtask 4 with the SCRF. Following the questionnaires, these three preferred to fly with the PRF-CRF and did not collide when using this configuration. So while the PRF-CRF is generally desired, the SCRF has a more selective group of supporters. This is noticeable in the CARS plot, Figure 29, where the SCRF had two votes below a score of 6 but the same amount of votes as the PRF-CRF for the scores of 8 and 9.

Finally, the research question was whether or not an additional visualization could be used to improve the acceptance of this haptic interface which is also the last hypotheses. The CARS result showed no significant effect, but did reveal a slightly better acceptance score for both visualizations. This can be correlated to the acceptance questionnaire where all participants had a preferred configuration, namely one of the visualization. This result means that the goal of this research has been accomplished, which was to raise the acceptance of the haptic system. Furthermore, this was done without worsening the measures as safety, performance and workload. While this does not statistically prove that the visualizations did improve the acceptance, future research might be able to do this with several changes.

A. *Recommendations for Future Research*

The aim of this research was to improve the user acceptance of the HCAS. A thorough literature research was performed on why haptic interfaces have a low acceptance. The problem is that while the consensus of the system is often given, it differs greatly for each participant because acceptance is largely subjective. Therefore analyzing the user experience for each individual in an even more detailed level might reveal different acceptance problems with the current haptic interface. This way the visualization design can be made more user-friendly.

With the rise of virtual reality and high resolution video games, more advanced user interfaces are becoming a common requirement. Head up display designs from those applications might be useful to implement on the on-board camera view, an option that had been discarded in this research due graphical limitations. This way it is no longer necessary to look down on the navigation display when the camera view is obscured.

A recommendation for avoiding having almost no statistically significant results might be to increase the number of participants. Twelve participants provided very loosely spread data points, doubling the number of participants could be enough to eliminate this uncertainty. Using a small effect size f of 0.10 [24], twenty-four participants increase the power from 0.61 to 0.91 [25].

The human-in-the-loop experiment might yield better result by altering subtasks into a scenario that brings out the full potential of having an additional visualization. More open spaced subtasks or trajectories with multiple alternative paths can give interesting results. Participants can apply their control strategies on different scenarios which they think that benefits them most. This way the user experience can really be tested since operators might consider a totally different strategy when given the decision to alter their course instead of forcing them into the same flight path.

VII. Conclusions

The goal of this research was to design and evaluate newly designed visualizations to provide a better user acceptance for UAV teleoperator. The subjective results from the human-in-the-loop experiment which tested three different configurations, two with and one without additional visualizations, showed that additional visualizations were a welcome addition. It provided more clarity of the haptic feedback system and could be used to confirm the spatial awareness of the teleoperator. However, from the objective data is was shown that participants did not alter their control strategies when an additional visualization was provided. This resulted in marginal difference in measured metrics, the new designs did not improve but also did not deteriorate the operators safety, performance and workload. Overall there was no significant effect between the configurations.

This means that while the visualizations were appreciate and raised the acceptance of haptic system, evaluating such an interface would require a different human-in-the-loop experiment setup. The overall setup such as procedure and apparatus would still be sufficient but a change in subtask and environments would be necessary.

References

[1] K. E. Boon and D. C. Lovelace, "The Domestic Use of Unmanned Aerial Veiclesh," in *Terror. - Comment. Secur. Doc.* Oxford University Press, 2014, p. 215.

[2] K. W. Williams, "A Summary of Unmanned Aircraft Accident-Incident Data: Human Factors Implications," FAA The Defence Technical Information Center, Tech. Rep. December, 2004.

[3] T. B. Sheridan, "Human Enhancement and Limitation in Teleoperation," in *Teleoperation Robot. Sp.*, S. B. Skaar and C. F. Ruoff, Eds., 1994, pp. 43–86.

[4] J. S. McCarley and C. D. Wickens, "Human Factors Implications of UAVs in the National Airspace," in *Hum. Factors UAVs*. University of Illinois, 2005, pp. 6–10.

[5] M. H. Draper and H. A. Ruff, "Multi-Sensory Displays and Visualization Techniques Supporting the Control of Unmanned Air Vehicle," *IEEE Int. Conf. Robot. Autom.*, pp. 1–6, 2001.

[6] T. M. Lam, "Haptic Interface for UAV Teleoperation," Ph.D. dissertation, Delft University of Technology, 2009.

[7] B. H. Krogh, "A Generalized Potential Field Approach to Obstacle Avoidance Control," *Robot. Int. SME Conf.*, no. MS84-484, pp. 1–15, 1984.

[8] D. A. Abbink, M. Mulder, and E. R. Boer, "Haptic Shared Control: Smoothly Shifting Control Authority?" *Cogn. Technol. Work*, vol. 14, no. 1, pp. 19–28, 2011.

[9] P. G. Griffiths and R. B. Gillespie, "Sharing Control Between Humans and Automation Using Haptic Interface: Primary and Secondary Task Performance Benefits," *Hum. Factors*, vol. 47, no. 3, pp. 574–590, 2005.

[10] C. Borst, F. H. Grootendorst, D. I. K. Brouwer, C. Bedoya, M. Mulder, and M. M. van Paassen, "Design and Evaluation of a Safety Augmentation System for Aircraft," *J. Aircr.*, vol. 51, no. 1, pp. 12–22, 2014.

[11] B. D. Seppelt and J. D. Lee, "Making adaptive cruise control (ACC) limits visible," *Int. J. Hum. Comput. Stud.*, vol. 65, no. 3, pp. 192–205, 2007.

[12] J. K. Kuchar and A. C. Drumm, "The Traffic Alert and Collision Avoidance System," *Lincoln Lab. J.*, vol. 16, no. 2, pp. 277–296, 2007.

[13] H. W. Boschloo, T. M. Lam, M. Mulder, and M. M. van Paassen, "Collision Avoidance for a Remotely-Operated Helicopter Using Haptic Feedback," *IEEE Int. Conf. Syst. Man Cybern. Collis.*, pp. 229–235, 2004.

[14] J. M. Kolsteeg, J. Smisek, M. M. van Paassen, and M. Mulder, "Haptic Interface for UAV Teleoperation - Changing Haptic Control Device Stifness based on Environmental Constraints," *TU Delft, Unpubl.*, pp. 1–15, 2014.

[15] E. Sunil, J. Smisek, M. M. van Paassen, and M. Mulder, "Tuning of a Haptic Collision Avoidance System for Unmanned Aircraft Teleoperation," *TU Delft, Unpubl.*, pp. 1–24, 2014.

[16] Daimler AG, "Mercedes-Benz Intelligent Drive," 2016. [Online]. Available: https://www.mercedes-benz.com/en/mercedes-benz/innovation/mercedes-benz-intelligent-drive/

[17] Tesla, "Tesla Autopilot," 2016. [Online]. Available: https://www.tesla.com/presskit/autopilot

[18] Volvo, "Volvo Intellisafe," 2016. [Online]. Available: http://www.volvocars.com/us/about/our-innovations/intellisafe

[19] J. Ellerbroek, K. C. R. Brantegem, M. M. van Paassen, and M. Mulder, "Design of a Co-Planar Airborne Separation Display," *IEEE Trans. Human-Machine Syst.*, vol. 43, no. 3, pp. 277–289, 2013.

[20] Frontier, "Elite Dangerous Gameplay," 2016. [Online]. Available: https://www.elitedangerous.com/en/gameplay/

[21] LucasArts Entertainment Company, "Star Wars Rogue Squadron II: Rogue Leader," 2001. [Online]. Available: http://www.lucasarts.com/products/rogueleader/

[22] S. G. Hart and L. E. Staveland, "Development of NASA-TLX (Task Load Index) - Results of Empirical and Theoretical Research," *Adv. Psychol.*, vol. 52, no. C, pp. 139–183, 1988.

[23] K. K. Lee, "Development and Validation of the Controller Acceptance Rating Scale (CARS)," *4th USA/Europe Air Traffic Manag. R&D Semin.*, p. 14, 2001.

[24] J. Cohen, "F Tests on Means in the Analysis of Variance and Covariance," in *Stat. Power Anal. Behav. Sci.* New York: Academic Press, 1977, pp. 273–406.

[25] F. Faul, E. Erdfelder, A. Buchner, and A. Lang, "Statistical Power Analyses using G*Power 3.1 - Tests for Correlation and Regression Analyses," *Behav. Res. Methods*, vol. 41, no. 4, pp. 1149–60, 2009.

Part II

Book of Appendices

Appendix A

Literature Study on Acceptance of Automation

The aim of this literature research was to find viable solutions to improve the acceptance of automation problem. Two different studies will be held to identify suitable methods, being general acceptance of automation and state of the art solution.

A-1 Definition of Acceptance of Automation

To understand more on how the acceptance of automation problem plays a role in the engineering world, research on problems of automation itself should be studied. As said in the introduction, automation is usually needed in cases where the human capabilities are lacking or given tasks are too hazardous (Wickens, Lee, Liu, & Becker, 2004). Parasuraman has written many papers regarding the advantages and disadvantages of automation (Parasuraman & Riley, 1997; Parasuraman, Sheridan, & Wickens, 2008; Parasuraman & Wickens, 2008). Furthermore according to these papers, automation varies in different levels, with higher levels representing increasing machine autonomy being called Level of Automation (LoA). In cases with human-machine interaction, or for this research shared control, the common problems are misuse and disuse of automation (Parasuraman & Riley, 1997). Relating these problems back to the teleoperation task, several misuses and disuses can be identified (Parasuraman & Riley, 1997):

- Lack of information/knowledge: Operators have often trouble understanding on how the automation functions. This lack of knowledge of the system has sever consequences on the attitude towards the automation. It directly relates to the trust and reliance on the automation.
- Behavioral adaption: This falls under over reliance on automation as an aspect of misuse. If the operator has too much trust in a system, it might give decision biases that can lead to incorrect actions.

- Disuse of automation: If there is a distrust in the automation system, because the operator believes it is not reliable or just dislikes the new system, it can lead to ignoring the automation or even disabling the the automation.

These three problems are a few of the many other problems that influence the acceptance of automation (Parasuraman & Riley, 1997). While there are more points that are related to the acceptance, for shared control these problems are also identified from other related researches (Lam, 2009; Seppelt & Lee, 2007; Borst et al., 2014).

A-2 Improving the Acceptance of Automation

Improving the acceptance of automation is no easy task. Especially if research states that unreliable automation can lead to significant reduction in performance (Wickens, Dixon, & Ambinder, 2006). This means that perfect automation is needed to increase the acceptance since as mention section A-1 users lose trust if a system is not reliable. Since perfect automation is still not possible, a different approach is needed to improve the acceptance.

Referring back on the LoA, several studies has shown that unless perfect reliability can be ensured, a high LoA decision automation might be risky if the process involves human safety. High levels of trust in these systems that are not perfectly reliable might lead to over reliance and failure to monitor low-level information sources that provide data to the automation. Therefore having high automation does not equal better results. Having a lower LoA which gives information on suggested actions instead of taking decisions provides better performance in some human-machine environments since the operator continue to generate different course of actions with the low-level information that is available. This as a result gives the user more awareness of the the consequences of the choice and of the choice that might be incorrect because of faulty automation (Parasuraman & Wickens, 2008). Therefore this approach can similarly be used for improving the Unmanned Aerial Vehicle (UAV) haptic interface. While the LoA is not lowered, by providing the user additional information the operator is more aware of the automation.

A-3 State-of-the-Art Research on Acceptance of Automation

For this research, a visualization has to be made for an existing haptic interface. It is useful to know if there are similar cases where researchers wanted to improve the acceptance of an automated system using haptic feedback by adding visualizations.

A similar case was investigate by (Seppelt & Lee, 2007). In this paper further research was done on the human-machine interaction of Adaptive Cruise Control (ACC). It was shown that the driving safety was compromised if the drivers did not understand how the ACC functioned. By applying Ecological Interface Design (EID) to create a visualization of ACC behavior, they intended to promote appropriate reliance and support effective transitions between manual control and ACC. The display featured the state of the ACC, giving certain signals when the braking algorithm limits were exceeded or/and sensor failures. One of the display concepts is shown in Figure A-1a. The results of the EID display were that users relied more on the cruise control when the display was presented than when it was not, proactively deactivating the ACC. With the display on the braking responses of the users were faster and more consistent when braking limits were exceeded. Even in manual control, the EID display reduced the driver's workload in low visibility scenarios. Furthermore it stated that providing users with continues information on the status showed better results than when only warnings were issued to the user if a failure occurred.

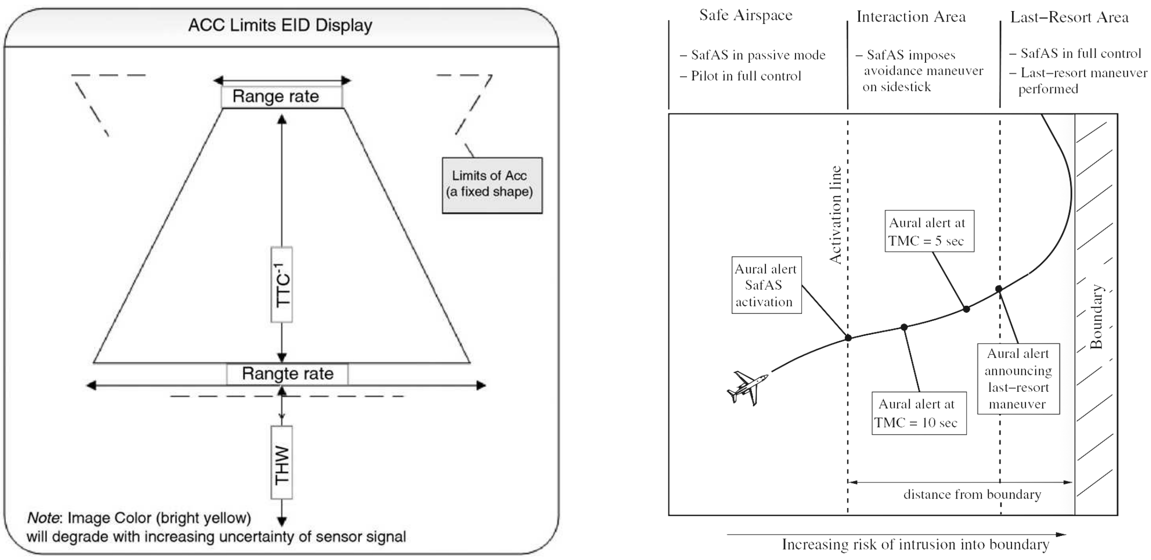

(a) EID display of the Adaptive Cruise Control

(b) Pictorial representation of the SafAS

Figure A-1: Examples of both shared control EID research (Seppelt & Lee, 2007) (Borst et al., 2014)

Another similar case was investigate by (Borst et al., 2014). The haptic interface system, called Safety Augmentation System (SafAS), was developed to let commercial airline aircraft pilots feel force feedback when approaching no-fly zones. The force feedback would then prevent the aircraft from entering this area. A pictorial representation can be seen in Figure A-1b. The results stated that while the pilots did appreciate the haptic feedback they received, less than half of the participant found the force feedback easy to understand. Lack of information on how and when the haptic feedback system activated was the main concern of the pilots. Extra visual feedback is commonly used as a solution and receive positive feedback from its users (Kuchar & Drumm, 2007). Adding additional visual cues indeed proved to increase the percentage of acceptance, however one of the visual design options that was tested caused more confusion because of redundant information and clutter.

Appendix B

Preliminary Force Field Visualization Design Options

In this chapter several preliminary options for the design of haptic feedback visualization were discussed. From these concepts two of them were analyzed and tested using off-line simulations before implementing them for use in the human-in-the-loop experiments. The designs are to be used on the Navigation Display (ND) of the cockpit, overlaying the current display interface.

B-1 Force Field Visualization Design Options

As discussed in chapter A, there are many ways to change the interface to suit the workings of the haptic feedback. Finding the perfect visualization is a difficult and almost impossible since for every different scenario and person the preference will differ. Therefore a solution that satisfies the need for visualization in most situations and provides accurate results will be sufficient for the experiment.

In total there are six design options that are considered. Each of them have their own advantages and disadvantages but only four of them will have a more extensive analysis. A design option tree is seen in Figure B-1.

For all six of the concepts, two scenarios will be presented. The first scenario is when the UAV flies into an obstacle head on, while the second scenario is when the UAV tries to enter or enters a gap between two obstacles. A representation with risk vectors of the two scenarios can be seen in Figure B-2.

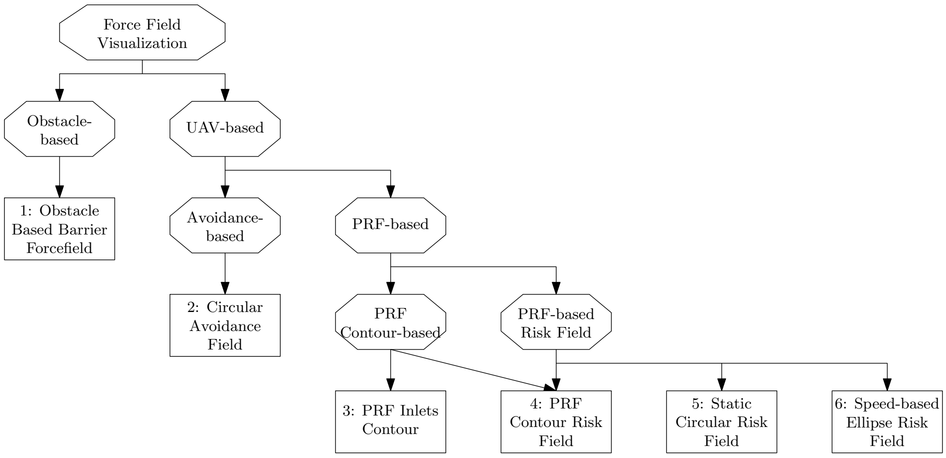

Figure B-1: Design option tree

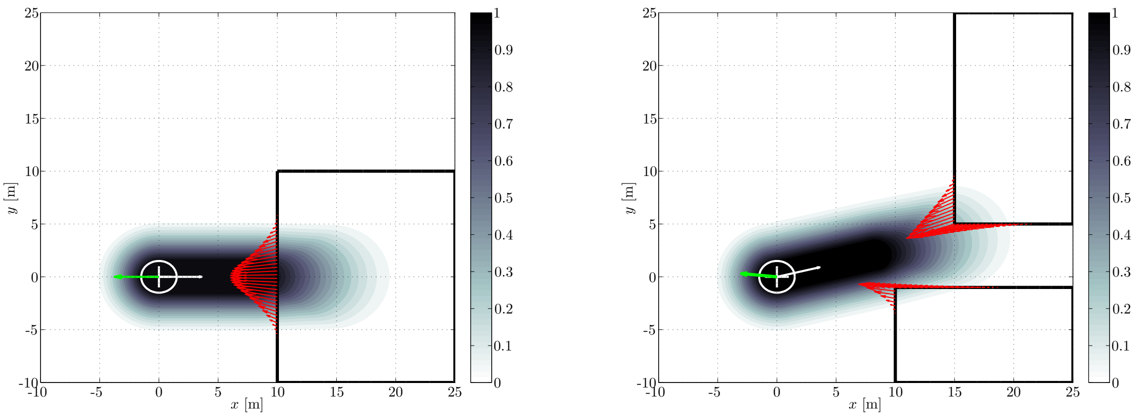

(a) One obstacle head-on scenario **(b)** Two obstacle gap scenario

Figure B-2: Two-dimensional contour plot of two different obstacle scenarios

B-1-1 Obstacle-Based Barrier Force Field

The Obstacle-Based Barrier Force Field (OBBFF) is the only concept that differs greatly from all other design options. The main difference is that instead of having a force field around the UAV, a force field is placed around the obstacle. An example of this concept is shown in Figure B-3a. The theory follows that when the vehicle touches the force field (barrier) of the obstacle, the operator will feel the haptic feedback. If the UAV continues along the same path, the operator will see that the barrier dents in and can expect more force on the stick as in Figure B-3b. Flying away from the obstacle will undent the barrier and no force will exerted on the stick.

This concepts advantage is that the operator can easily expect when the force feedback kicks in. Simply avoiding the barrier means that no force will be exerted and steering away from the barrier means less force. However, there are several major disadvantages to this concept. The biggest problem occurs when multiple obstacles are present. The barriers that these obstacles have will overlap with each other. This situation can be seen in Figure B-4. It is unclear for

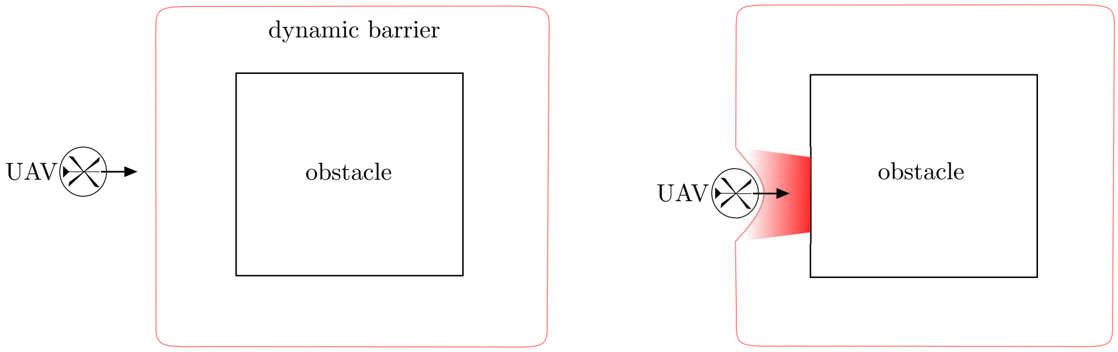

(a) UAV outside risk zone **(b)** UAV entering risk zone

Figure B-3: Obstacle-Based Barrier Force Field in head-on scenario

the operator to see how the force on the stick is created since both of the barriers are dented. Another problem is that Parametric Risk Field (PRF) is dependent on speed which in turn affects the barrier around the obstacle. Having a high speed results in a large barrier while at very low speed almost no barrier is visible. Flying through these ever changing barriers is a very tiresome and unpredictable task. The PRF algorithm is simply not meant to be applied on the obstacles. Therefore this concept is discarded and no longer a viable option.

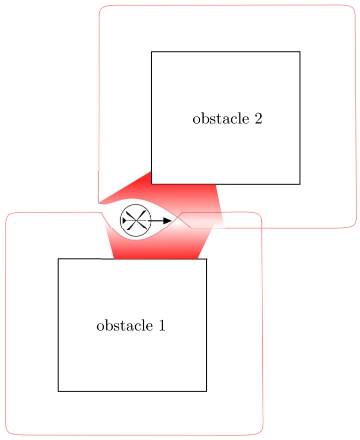

Figure B-4: Obstacle-Based Barrier Force Field in gap scenario

B-1-2 Circular Avoidance Field

The Circular Avoidance Field (CAF) is based on the same principal as the Solution Space Diagram (SSD) as discussed in section A-3. In this design an circular area around the UAV presents an avoidance field. The outer boundary of the circle states the maximum velocity of the vehicle while the inner circle means zero velocity. A speed vector inside this area gives the current speed and heading of the UAV. If a certain speed and heading combination results in a collision with an obstacle, it will be visible within this avoidance field. Meaning that the pilot has to make sure the speed vector does not overlap with this area. Since an overlap of the speed vector with this critical area results in collision, the haptic feedback will activate before the operator can steer into this direction. Thus a gradient is applied in the avoidance field so that the operator knows that with a certain speed and heading a force will already act on the stick. This gradient is clearly visible in Figure B-5a.

An advantage of this concept is that the pilot knows directly in which direction and with what speed the UAV can steer without colliding. It is however very difficult to see when flying at high speed and very close to the buildings. It also does not give enough information about the force feedback since it suffers the same problem with multiple obstacles like with the OBBFF. This problem can be seen in Figure B-5b. It is also very unclear for the pilot if a small corridor is large enough for the vehicle since the gradients almost overlap in these areas. This concept is therefore also discarded.

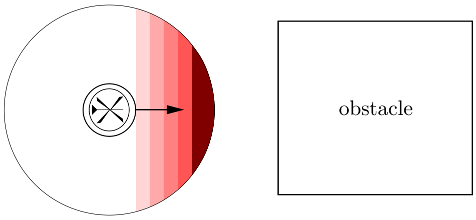

(a) Circular Avoidance Field in head-on scenario

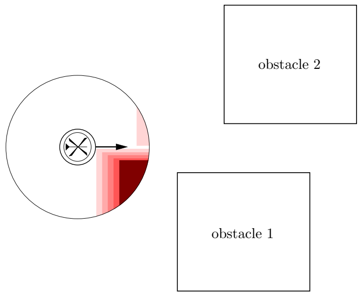

(b) Circular Avoidance Field in gap scenario

Figure B-5: Circular Avoidance Field scenarios

B-1-3 PRF Inlets Contour Field

The PRF Inlets Contour Field (PRF-ICF) is a design that uses the geometry of the PRF. It takes the most outer boundary of the risk field and displays it on the ND. When there are no obstacles, the PRF-ICF looks just like the normal PRF seen in Figure B-2a except that it only display the outer contour. This can be seen in Figure B-6.

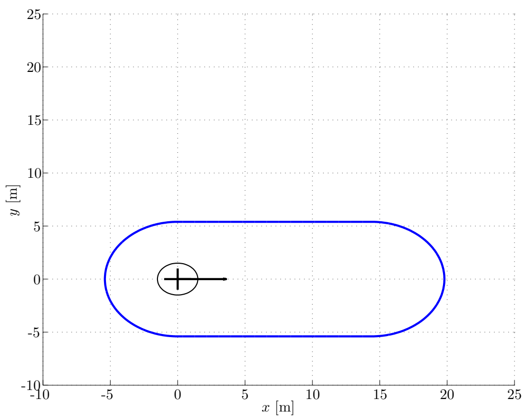

Figure B-6: Outer contour of Parametric Risk Field

When the UAV approaches an obstacle, the outer contour dents in and creates inlets, similar as the OBBFF. The risk vectors as can be seen Figures B-2a and B-2b are used to create these inlets. The direction and size are both determined by the PRF functions, however they are scalable so that they can create smaller or larger inlets. The results of this method can be seen in Figure B-7.

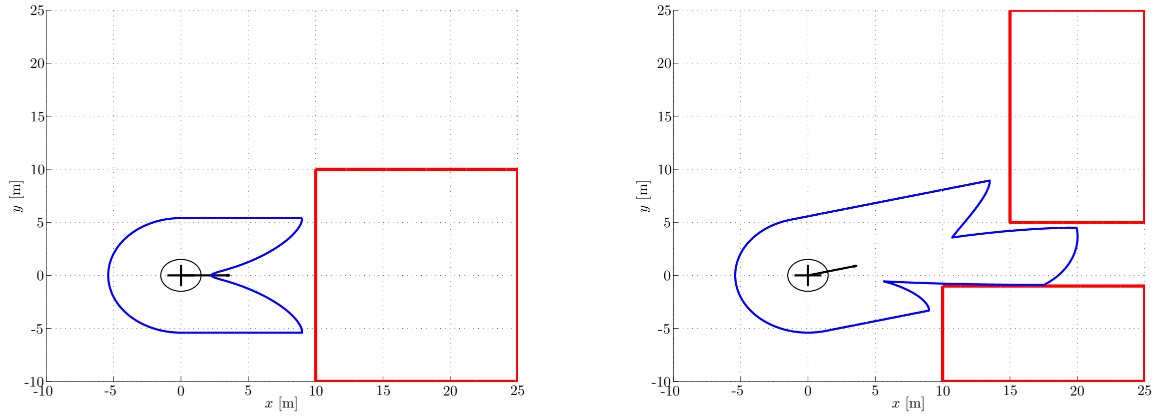

(a) One obstacle head-on scenario

(b) Two obstacle gap scenario

Figure B-7: PRF Inlets Contour Field in two different scenarios

The main advantage of this method is that the operator can see when to expect force feedback. If the outer boundary touches an obstacle, a small force will be generated simultaneously with an inlet in the contour field. Because the outer boundary changes accordingly with the speed, the pilot knows precisely at different speeds when the force feedback activates. There are however some drawbacks with this concept. Again as the previous designs, multiple obstacles result in many inlets. This can be very confusing if there are obstacles in multiple directions because the inlets do not state how exact the final risk vector behaves. The PRF-ICF gives inlets of all risk vectors even though some do not contribute to the final risk vector. Another problem is that although the inlets are scalable, it does not let the operator see the minimum separation distance of the "protected zone". Without knowing the limit, the pilot might think that some flight paths are not possible while still experiencing only mild force feedback. Hence this concept is not viable for future experiment.

B-1-4 PRF Contour Risk Field

The PRF Contour Risk Field (PRF-CRF) is based on the same theory of the PRF. However instead of the entire risk field, the original PRF boundary like with the PRF-ICF and the area that overlaps with the obstacle is shown. This means that when the outer boundary overlaps with an obstacle, the risk fields appear. Since the length of the boundary is now tied with the speed as with the PRF algorithm, the operator knows exactly when the force feedback activates. An example of the PRF-CRF is shown in Figure B-8.

A disadvantage of this concept is that a large space of ND might be covered with the risk visualization. Especially when flying at a higher speed, the PRF contour increases greatly in

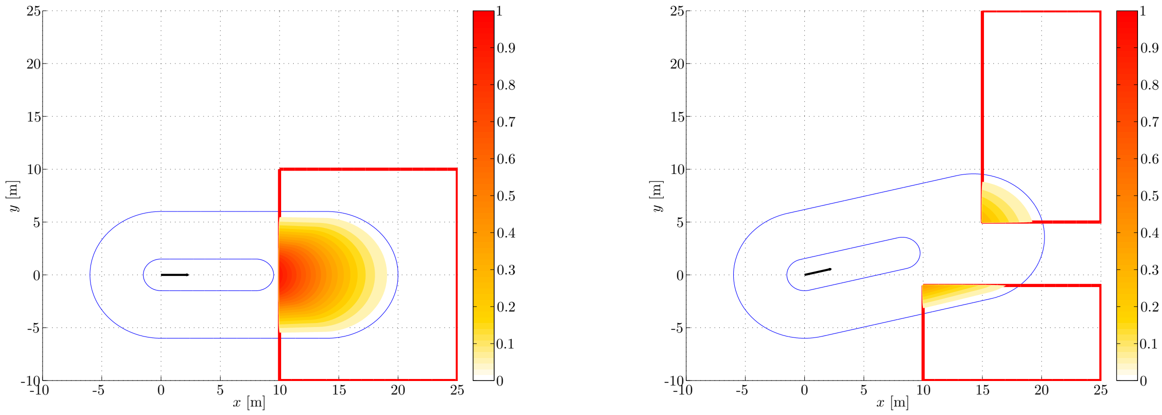

(a) One obstacle head-on scenario

(b) Two obstacle gap scenario

Figure B-8: PRF Contour Risk Field in two different scenarios

length. It might cover up any upcoming obstacles or any other important information on the ND. However since the operator also has a camera view of the outside visuals, this might not give any serious problems. This concept will therefore be included in the next research phase.

B-1-5 Static Circular Risk Field

The Static Circular Risk Field (SCRF) is the second of the three concepts that displays a risk field. The method behind this concept is that it area surrounding the UAV has and inner and outer boundary similar as CAF. The outer boundary represents the minimum risk 0 and the inner boundary the maximum risk 1. For the SCRF both of these boundaries are circles that can be predefined. Since the risk vectors of the PRF are pointing to the center of the vehicle with a certain risk value, they can be translated to an angle and position within these boundaries. If all risk vectors are plotted within this area, the pilot knows in which heading the largest risks are including those who contribute to the force feedback. In Figure B-9 this concept is seen in both scenarios with one and two obstacles.

With this concept, the operator can see how much and from which direction the force feedback comes from. The highest risk value and the direction indicate which side the operator has to steer to avoid the obstacle. Gaps that occur inside this circular area can indicate a possible passage as depicted in Figure B-9b. A major disadvantage of this method is that the operator cannot see how the PRF works in relation to the speed of the UAV. Problems may occur when the UAV flies to an obstacle at high speed and slows down because of the force feedback. However when the vehicle slows down, the risk values also lessen and no risk values could be shown if the obstacles are still far away. Accelerating in the same flight path again might suddenly reveal high risk values since the UAV is now closer to the obstacle and cause confusion to the pilot. Even with this minor problem, it might be a possible candidate for the human-in-the-loop experiment and thus will be used in the next research phase.

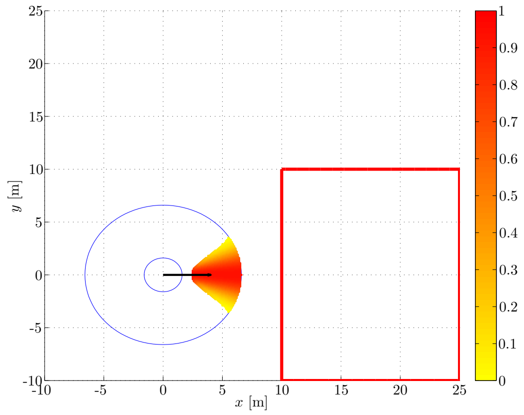

(a) One obstacle head-on scenario

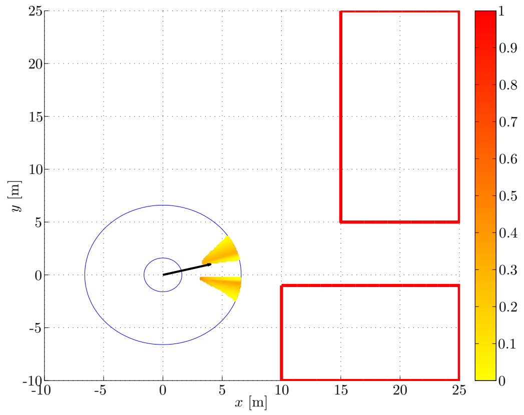

(b) Two obstacle gap scenario

Figure B-9: Static Circular Risk Field in two different scenarios

B-1-6 Speed-Based Ellipse Risk Field

The Speed-Based Ellipse Risk Field (SELRF) concept uses the same algorithm as the SCRF except that the geometry of the outer boundary is defined differently. While the SCRF uses a circle as inner and outer boundary, the SELRF has an elliptic boundary in the flight direction of the UAV. By letting the semi-major axis of the ellipse scale with the vehicle speed, the outer boundary becomes dynamic. Figure B-10a shows the effect of using a speed-based ellipse. Having the outer boundary bound to the UAV speed, it gives the operator a better feeling when force feedback is expected. Compared to the SCRF the risk field area also becomes larger making it easier to see how high the risk is as seen in Figure B-11.

A downside of the elliptic boundary is that the length of the semi-major axis is not equal to the PRF outer boundary length. This means that if an obstacle is inside the PRF boundary and thus creating a force feedback, it does not necessary mean that the ellipse also overlaps with the obstacle. This might confuse the operator since it would be expected that an overlap with the obstacle means a certain risk. This problem can be seen in Figure B-10b. This concept could also be a possible candidate for the experiment but due limitations of both software and hardware capabilities of Delft University Environment for Communication and Activation (DUECA) in combination with the current simulation code it was decided not to include this concept.

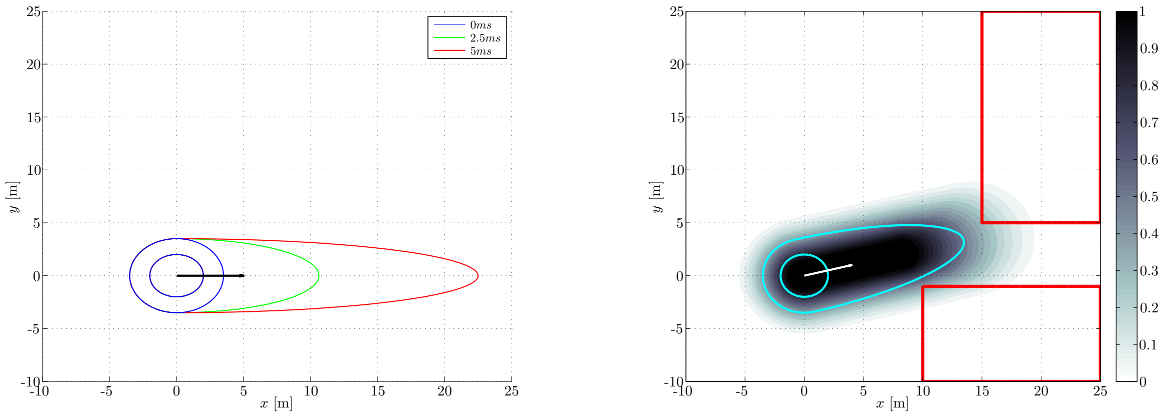

(a) SELRF with increasing UAV speed

(b) Contour of SELRF with associated PRF

Figure B-10: Speed-Based Ellipse Risk Field method overview

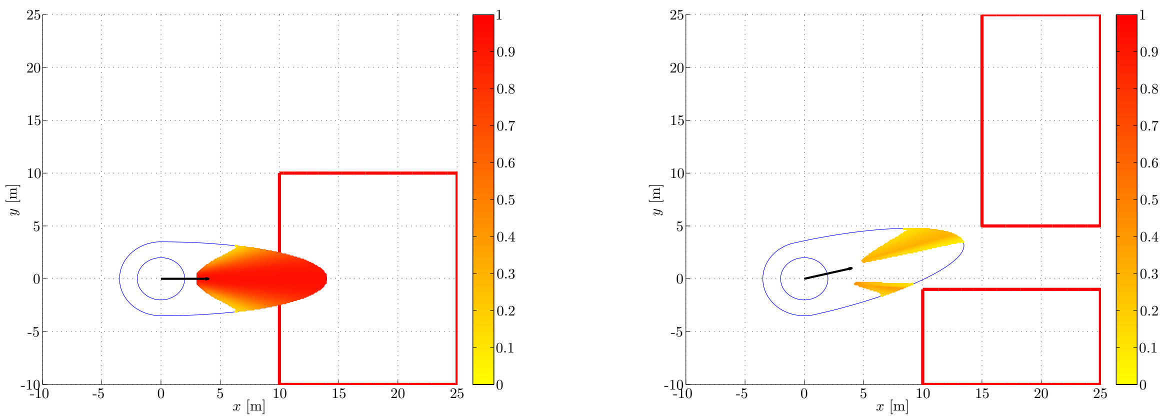

(a) One obstacle head-on scenario

(b) Two obstacle gap scenario

Figure B-11: Speed-Based Ellipse Risk Field in two different scenarios

Appendix C

DUECA UAV Teleoperations Structure

The human-in-the-loop experiment uses DUECA to simulate a UAV Teleoperation environment. This teleoperation environment was developed by M.M. van Paassen and has currently been used for many research. For this research project, a revised version of the environment was modified. Several modules has been changed and added to the project to include the experimental visualizations. The revised version was previously used by (Lam, Boschloo, Mulder, Paassen, & Helm, 2004), (Sunil, Smisek, Paassen, & Mulder, 2014) and (Kolsteeg, Smisek, Paassen, & Mulder, 2014).

In this chapter all modules in the project are briefly explained, section C-1 and C-2, and the simulation architecture visualized by a flowchart, section C-3. Because of the complexity of the architecture, the flowchart has been split in five parts. The structure of the flowcharts is as follows: In the left column all 26 modules are listed and their output channels are displayed in the middle column. The right column states the input modules with their associated channels. In the chart the modules noted in blue are borrowed modules while green modules are redundant modules which are not used in this experiment.

C-1 Created and Copied Modules

AFFVisual - *Ground Station Module* - Main development module, here all relevant files for both visualizations on the ND of the experiment are calculated and generated. This module replaces the old "NavDisplay" module.

CamDisplay - *Ground Station Module* - Generates the on-board camera view display.

CamDownlink - *Ground Station Module* - Converts the helicopter camera data to useable format for the "CamDisplay" module.

CASDisplay - *Redundant Ground Station Module* - Old module of Lams project that is no longer used and works. Should have been able to visualize the obstacle detection range.

DataLogger - *Ground Station Module* - As the name states, logs all relevant data that is selected.

DelayedDataLogger - *Redundant Ground Station Module* - Old module of Lams time-delay experiment. Logged the additional delay data.

HapticCAS - *Ground Station Module* - Main module for calculations of the haptic feedback based on the risk fields.

HeliCam - *Helicopter Module* - Uses the helicopter state data from the “UAVHeli” module to generate the camera view.

HeliDownlink - *Helicopter Module* - Converts the helicopter telemetry data from the helicopter sensors to useable formats.

HeliSensors - *Helicopter Module* - Defines the sensors that are available on the helicopter. Includes the obstacle detection sensor.

HeliUplink - *Helicopter Module* - Converts control-stick inputs and other input signals to useable formats for the “UAVHeli” module.

NavDisplay - *Redundant Ground Station Module* - Generates a top-down view of the simulated UAV. Is now replaced by the “AFFVisual” module.

osgInclude - *Atmosphere Module* - One of the main graphics modules and is part of the OpenSceneGraph (OSG) modules. Here all the graphics world data is presented. Positional and graphical data of smoke plumes, building and miscellaneous objects are defined here.

ScenarioManager - *Ground Station Module* - Main module that is used as control panel. It generates all the initial conditions/settings including scenario selection.

SendQFeel - *Atmosphere Module* - Used for sending feedback to the HMILab hapic system.

SendWaves - *Redundant Atmosphere Module* - Old modules of Lams time-delay experiment. Uses the Wave Variable Technique.

Sound - *Ground Station Module* - This modules generates a sound when a collision occurs. Also includes the waiting time penalty for collisions.

UAVHeli - *Ground Station Module* - Main modules of the UAV helicopter. UAV model and dynamics are implemented here.

WaveMaster - *Redundant Atmosphere Module* - Old module of Lams time-delay experiment. Uses Wave Variable Technique. Master part of the master-slave system.

WaveSlave - *Redundant Atmosphere Module* - Old module of Lams time-delay experiment. Uses Wave Variable Technique. Slave part of the master-slave system.

WorldDisplay - *Redundant Atmosphere Module* - Old module that was part of the OSG modules. Module used to display the world with a default viewer.

C-2 Borrowed Modules

CSControlLoading - *HMILab Module* - Module for the haptics system.

HMILabSound - *HMILab Module* - Generates sound for the HMILab.

MultiStick - *HMILab Module* - Control-stick definition.

UAVVisualUpdate - *Redundant Module* - The revised and previous project of the UAV haptic interface research. The current simulation is based on this project and was used for initialization.

WorldView - *Atmosphere Module* - Graphics module that is part of the OSG modules.

C-3 Simulation Architecture Flowcharts

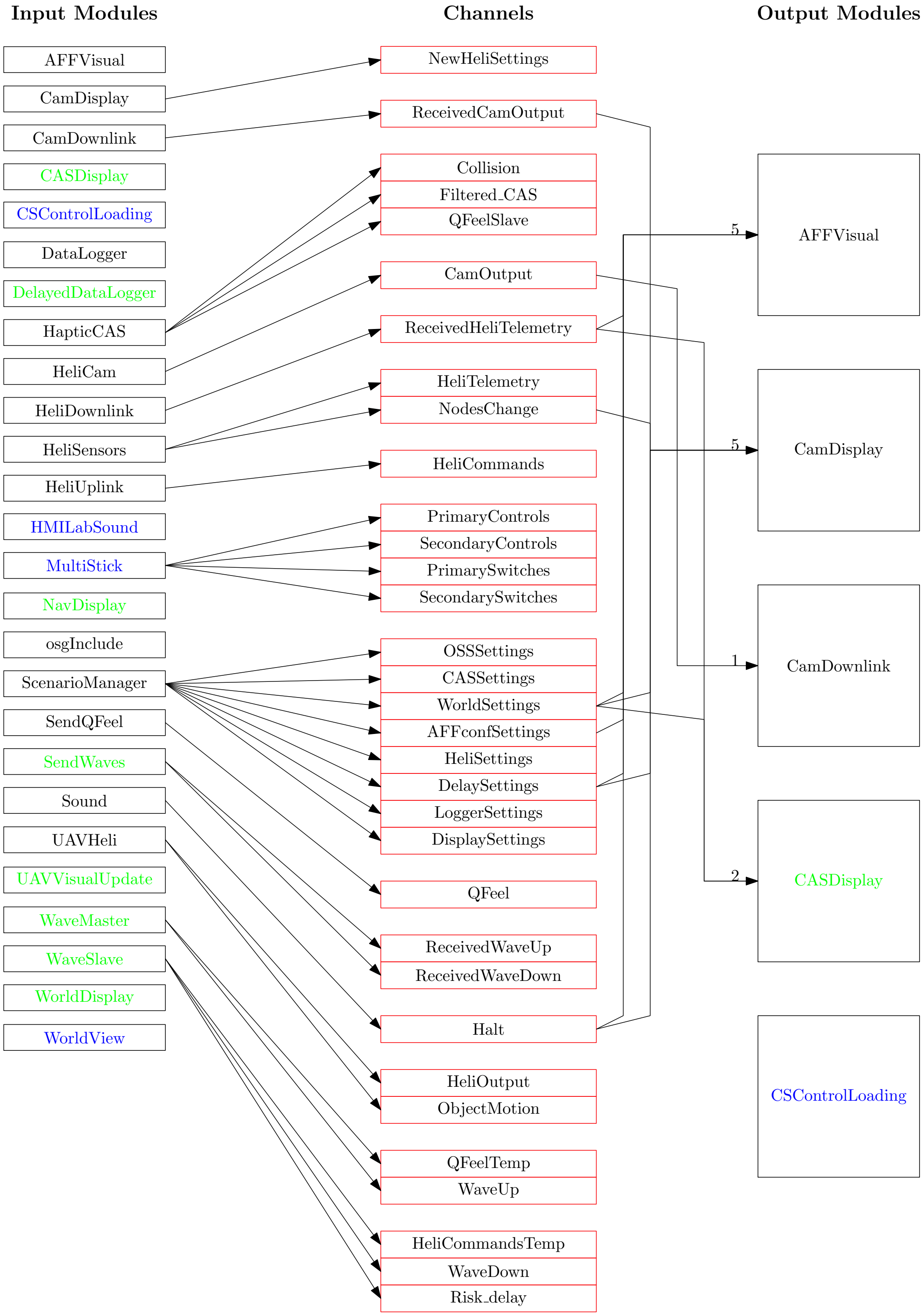

Figure C-1: Simulation Architecture Flowchart - Part 1

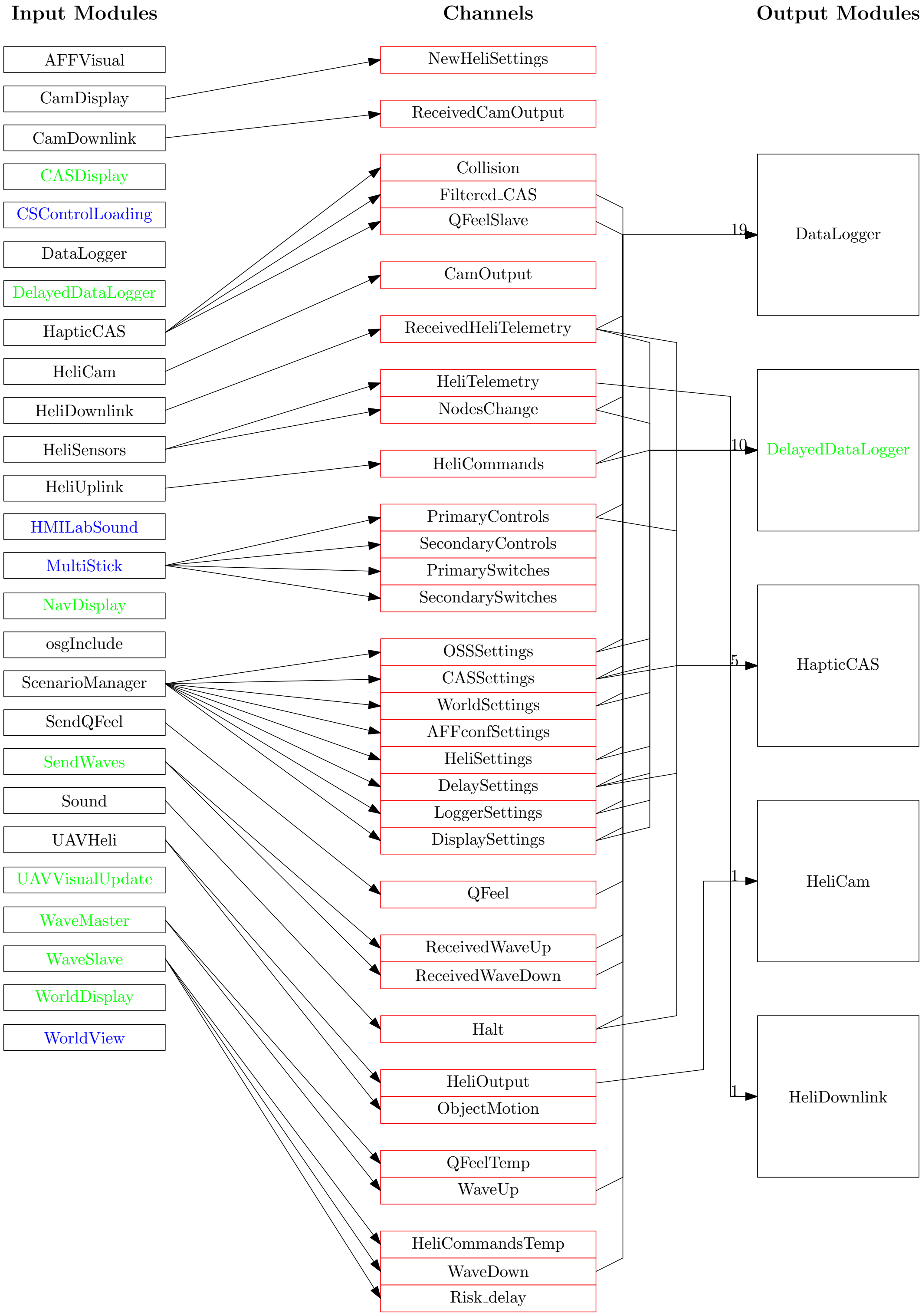

Figure C-2: Simulation Architecture Flowchart - Part 2

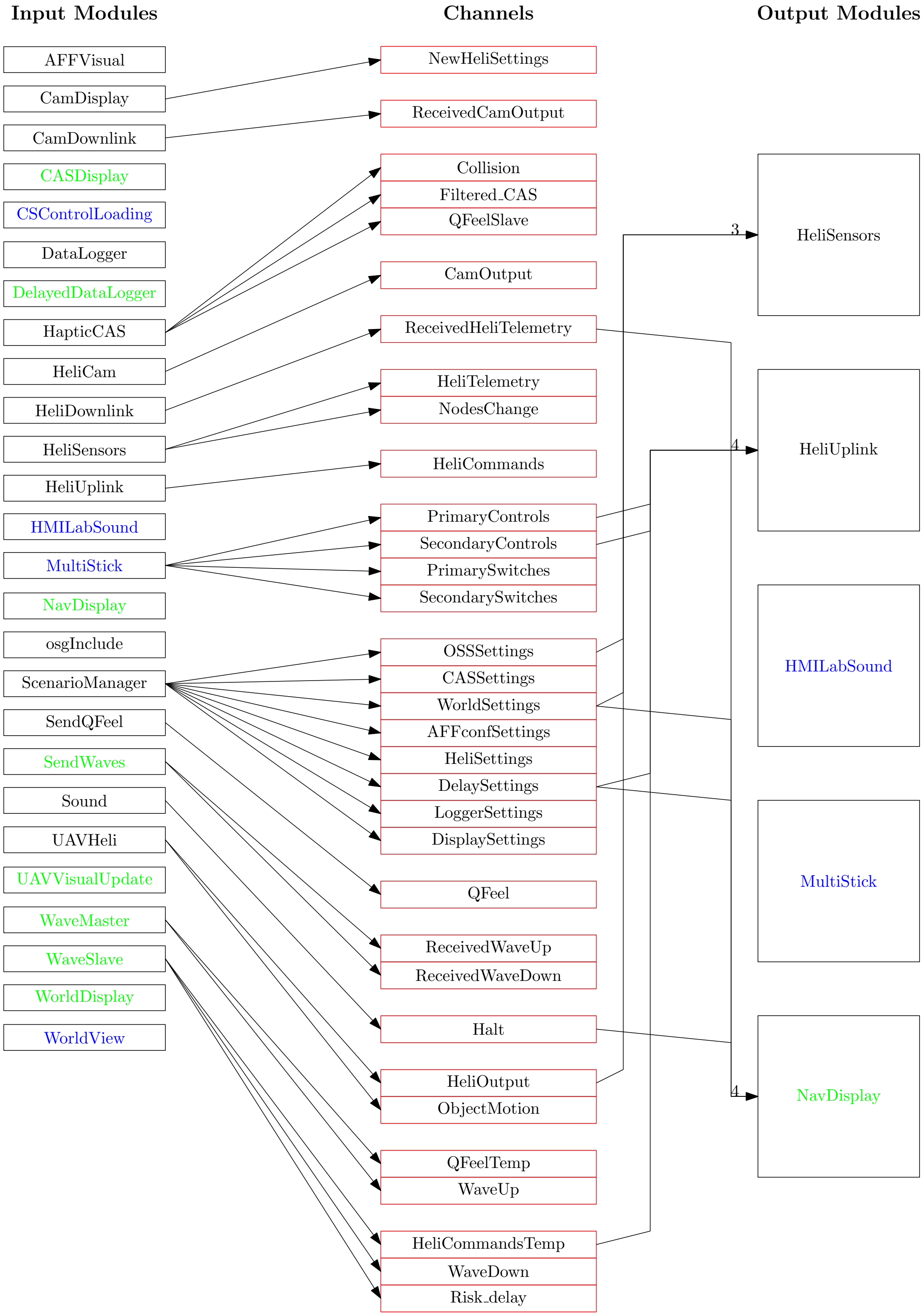

Figure C-3: Simulation Architecture Flowchart - Part 3

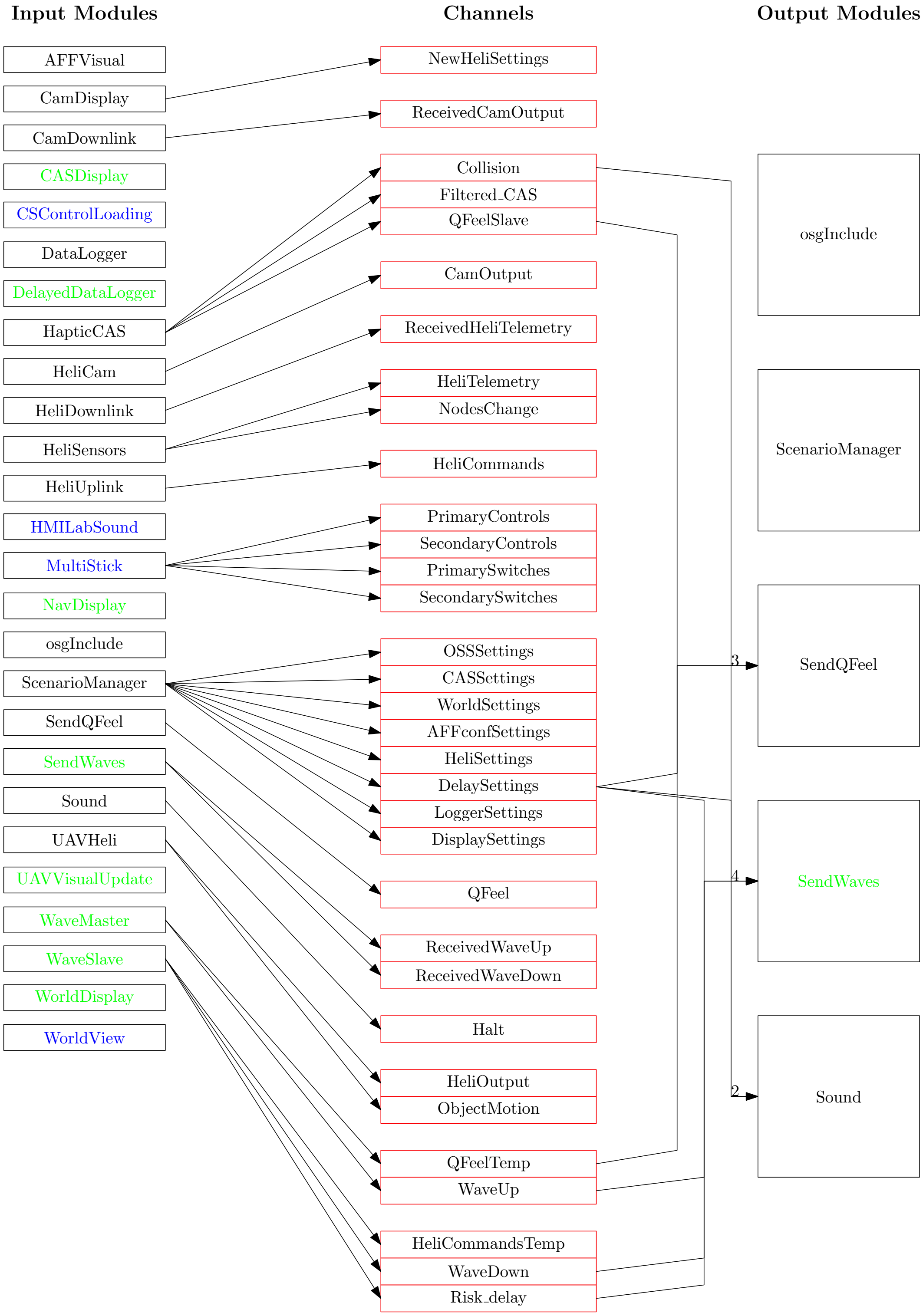

Figure C-4: Simulation Architecture Flowchart - Part 4

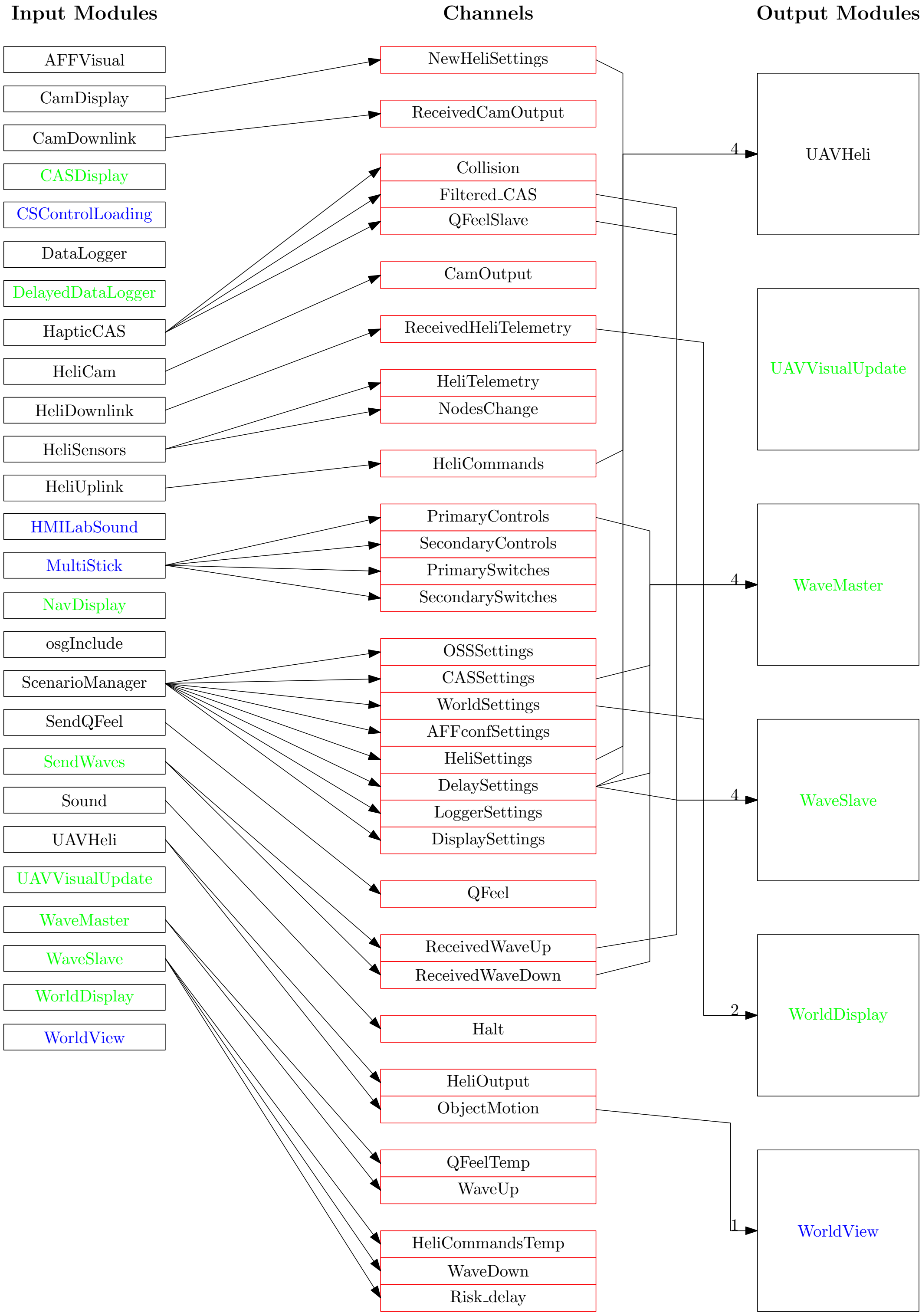

Figure C-5: Simulation Architecture Flowchart - Part 5

Appendix D

Experiment Briefing

The following pages show the pre-experiment briefing that the participants were asked to read before starting the experiment. This briefing was send out digitally by email one week before the planned experiment date.

Pre-Experiment Briefing

Visual Interface Design for a UAV Teleoperations Haptic Interface

I. Goal of the Experiment

The goal of this experiment is to evaluate the effect of additional visual feedback for UAV teleoperations on pilot acceptance, workload, safety and performance. This effect will be validated in the context of a collision awareness system for UAV teleoperations. This briefing contains a short overview of the experiment.

II. Experiment

2.1 Main Task

For this experiment you will be flying a simulated UAV by using a side stick as seen in Figure 1 (element 2). The altitude of the UAV is kept constant, so you only have control over forward and yaw motion. Your main tasks, in order of importance, will be to:

1. Complete the different trajectories while avoiding collision with any obstacles
2. While flying through the center of the smoke plumes on the ground
3. In the minimum amount of time

2.2 Trajectory

The trajectories that you will be flying are composed of six different sub-tasks arranged randomly in three different orders. Visualization will be provided on two displays. There is a camera image of the outside view on the projection screen in front of you and a navigation display with a top-down view. The smoke plumes also act as waypoints and are only visible on the outside view. When the UAV collides with an obstacle, the image will freeze for several seconds and a beeping sound will play from the loudspeakers. After several seconds your position will be reset to the start of the obstacle.

2.3 Conditions

In total three different conditions will be evaluated, with two conditions where an additional visual feedback is enabled on the navigation display and the third without any additional visual feedback, as can be seen in Table 1. Each condition will be tested thrice for each trajectory and will be presented to you in random order.

Table 1: Three different conditions on the navigation display

No Visual Feedback	Visual Configuration 1	Visual Configuration 2
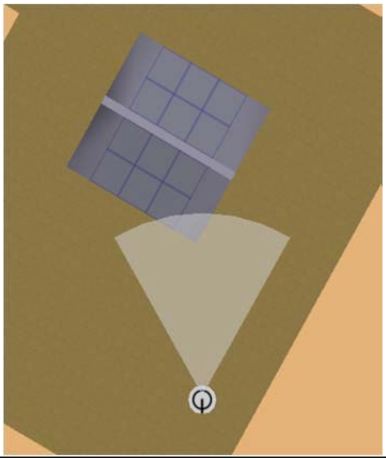	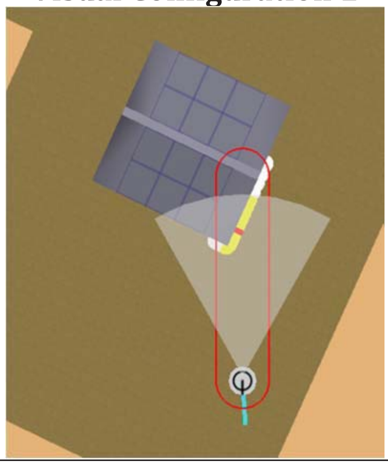	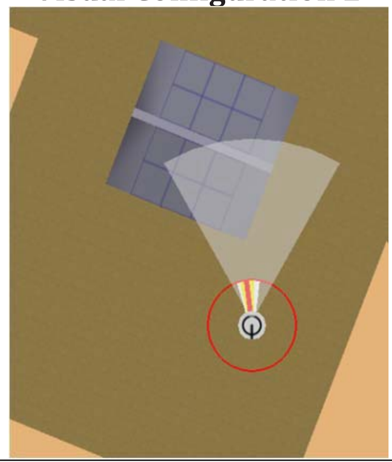

2.4 Procedure

The experiment will start with a set of training runs in order to familiarize yourself with the simulation environment and the haptic feedback system. During these runs we will also enable the additional visual feedback systems so you can get accustomed to the visuals. After these training runs, you will be asked if you are ready to start the measurement runs.

During the measurement runs, each of the three conditions will be repeated on all three trajectories. The conditions are presented in random order.

You may request to take breaks during the experiment in order to reduce fatigue. Furthermore, you are free to stop and withdraw from the experiment at any given time. The total experiment time including breaks and training is expected to be less than 2 hours.

2.5 Questionnaires

At the end of each condition, I will ask you to fill in a NASA Task Load Index (NASA-TLX) form, to get an indication of the general workload you experienced during that condition, together with a Controller Acceptance Rating Scale (CARS) form, which asks you to rate the automation support. Both can be found in the appendix of this pre-briefing.

Furthermore at the end of the experiment there is an additional questionnaire with some questions about your experiment experience and thoughts.

III. Location and Apparatus

The experiment will be conducted in the fixed-based flight simulator of the Human-Machine Interaction Laboratory (HMI-lab) at the Faculty of Aerospace Engineering. The lab is located in room 0.37 on the ground floor next to meeting room 3. The setup of the experiment is shown in Figure 2.

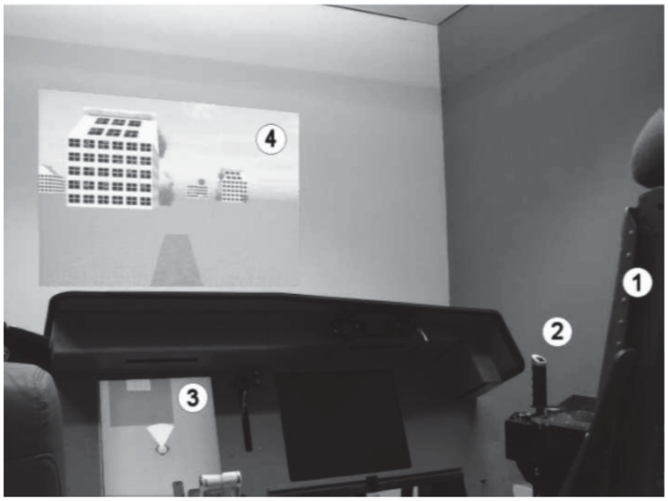

Figure 1 - Setup of the experiment room with seat (1), electro-hydraulic sidestick (2), navigation display (3) and on-board camera view (4). (Lam, Mulder, et al., 2009)

IV. Contact Details

If you have any questions or would like to have more information regarding the experiment, please do not hesitate to contact me on:

Email: V.Ho@student.tudelft.nl

Mobile: 06-41918521

Thanks for participating in this research!

Appendix E

Verbal Briefing Guide

The verbal briefing guide was used as reminder to consequently explain the same details about the experiment for all participants.

E-1 Before starting the experiment

1. Check if the participant has read the pre-experiment briefing and understood most of the instructions.
2. Ask participant to fill in consent form.
3. Mention that participant can always stop the experiment if necessary.

E-2 During the experiment briefing

1. Go over all the elements of the experiment briefing and spend more time if sections were unclear.
2. Explain clearly the priority of tasks, especially about not crashing.
3. Tell that there are three conditions and after each condition two questionnaire need to be filled in.
4. If breaks are needed, they need to speak up. Otherwise I will propose a break after the test runs.
5. Explain that I can give guidance and information while doing training runs, but during measurements runs not.

E-3 During training runs

1. Ask the participant to not touch the control stick during calibrations or/and when the system crashes.
2. When flying, check if the participants feels haptic feedback when nearing obstacles.
3. Let the participant crash into an obstacle and tell them to release the control stick and wait.
4. Mention to fly through the center of the (smoke)waypoints.
5. Make sure they understand how the current condition works before moving on to the next one.
6. Fill in the dummy questionnaire together and go over each element regarding this experiment.
7. Ask if there are any questions regarding the experiment and are acquainted with the system before holding a short break.

E-4 During measurements runs

1. Remind them that you can not help the participant but if system acts strangely, they can speak up.
2. Tell them when to fill in the forms when it is time.

E-5 After measurements runs

1. Ask them to fill in the questionnaire mindfully and mention that they can also interpret their experience verbally.
2. During individual subtask questions ask them not to switch back to the previous page after filling in one page.
3. After the questionnaires have been submitted and experiment has officially ended, ask for feedback about the experiment and if they liked it.

Appendix F

Experiment Scenarios

The human-in-the-loop experiment had in total three different trajectories for each configuration condition. In each of these trajectories, the same six subtasks are present. The scenarios for the measurement runs are listed in Table F-1. For the training runs, only Traj-1 was used for all three conditions.

Table F-1: Subtask order for three different trajectories

Trajectory	Subtask order
Traj-1	1-2-3-4-6-5
Traj-2	3-1-4-5-6-2
Traj-3	4-1-5-3-2-6

To minimize the effect of unwanted variability of the dependent variables, the three conditions were randomized using the 'Latin Square' method. There were three different configurations and three different trajectories. This meant that there are 36 possible combinations possible, however with only 12 participants it was decided to only alter the order of the conditions. The order with associated trajectories for each participant can be seen in Table F-2.

Table F-2: Order of conditions for each participant

Par. nr.	1st cond.			2nd cond.			3rd cond.		
1		*NV*			*PRF*			*SCRF*	
	Traj-1	Traj-2	Traj-3	Traj-1	Traj-2	Traj-3	Traj-1	Traj-2	Traj-3
2		*NV*			*SCRF*			*PRF*	
	Traj-1	Traj-2	Traj-3	Traj-1	Traj-2	Traj-3	Traj-1	Traj-2	Traj-3
3		*PRF*			*NV*			*SCRF*	
	Traj-1	Traj-2	Traj-3	Traj-1	Traj-2	Traj-3	Traj-1	Traj-2	Traj-3
4		*PRF*			*SCRF*			*NV*	
	Traj-1	Traj-2	Traj-3	Traj-1	Traj-2	Traj-3	Traj-1	Traj-2	Traj-3
5		*SCRF*			*NV*			*PRF*	
	Traj-1	Traj-2	Traj-3	Traj-1	Traj-2	Traj-3	Traj-1	Traj-2	Traj-3
6		*SCRF*			*PRF*			*NV*	
	Traj-1	Traj-2	Traj-3	Traj-1	Traj-2	Traj-3	Traj-1	Traj-2	Traj-3
7		*NV*			*PRF*			*SCRF*	
	Traj-1	Traj-2	Traj-3	Traj-1	Traj-2	Traj-3	Traj-1	Traj-2	Traj-3
8		*NV*			*SCRF*			*PRF*	
	Traj-1	Traj-2	Traj-3	Traj-1	Traj-2	Traj-3	Traj-1	Traj-2	Traj-3
9		*PRF*			*NV*			*SCRF*	
	Traj-1	Traj-2	Traj-3	Traj-1	Traj-2	Traj-3	Traj-1	Traj-2	Traj-3
10		*PRF*			*SCRF*			*NV*	
	Traj-1	Traj-2	Traj-3	Traj-1	Traj-2	Traj-3	Traj-1	Traj-2	Traj-3
11		*SCRF*			*NV*			*PRF*	
	Traj-1	Traj-2	Traj-3	Traj-1	Traj-2	Traj-3	Traj-1	Traj-2	Traj-3
12		*SCRF*			*PRF*			*NV*	
	Traj-1	Traj-2	Traj-3	Traj-1	Traj-2	Traj-3	Traj-1	Traj-2	Traj-3

Appendix G

Participant Consent Form

The following page shows the consent form that the participants were asked to sign before starting the experiment.

Subject Number:

Participant Consent From

Thank you for joining this research. As described in the briefing you have received, you will be participating in this experiment which last approximately 2 hours.

Any data collected today will be kept strictly confidential. You will never be identified in any way. There are no known risks or discomforts associated with your participation in this experiment. You have the right to stop the experiment anytime you wish.

By signing this consent form you confirm that you have read and understood its content and you agree to voluntarily participate in this simulation. You may request a copy of this form.

Date: ____________________________

Name: ___________________________

Signature: _________________________

Age: ______

Appendix H

Questionnaire

This chapter shows the questionnaires every participant had to fill in during and after the human-in-the-loop experiment.

The Controller Acceptance Rating Scale (CARS) form, section H-1, (Lee, 2001) and NASA Task Load Index (NASA-TLX) form, section H-2, (Hart & Staveland, 1988) were filled in after each experiment condition. The CARS provides additional subjective score on the acceptance of automation while the NASA-TLX shows the subjective workload rating.

After the measurement runs, the participants had to fill in a web-based questionnaire, section H-3, on the computer. The first four questions were ratings questions where the participant could select a value on a scale from 1-10 (Figures I-5a-I-5d). Afterward six individual subtask questions, section H-4, were provided in random order. The answers could be filled in as seen in Figure H-1e. Finally, three open questions were presented for the participant to answer (Figure H-1f).

H-1 CARS Form

Subject: Run:

Controller Acceptance Rating Scale

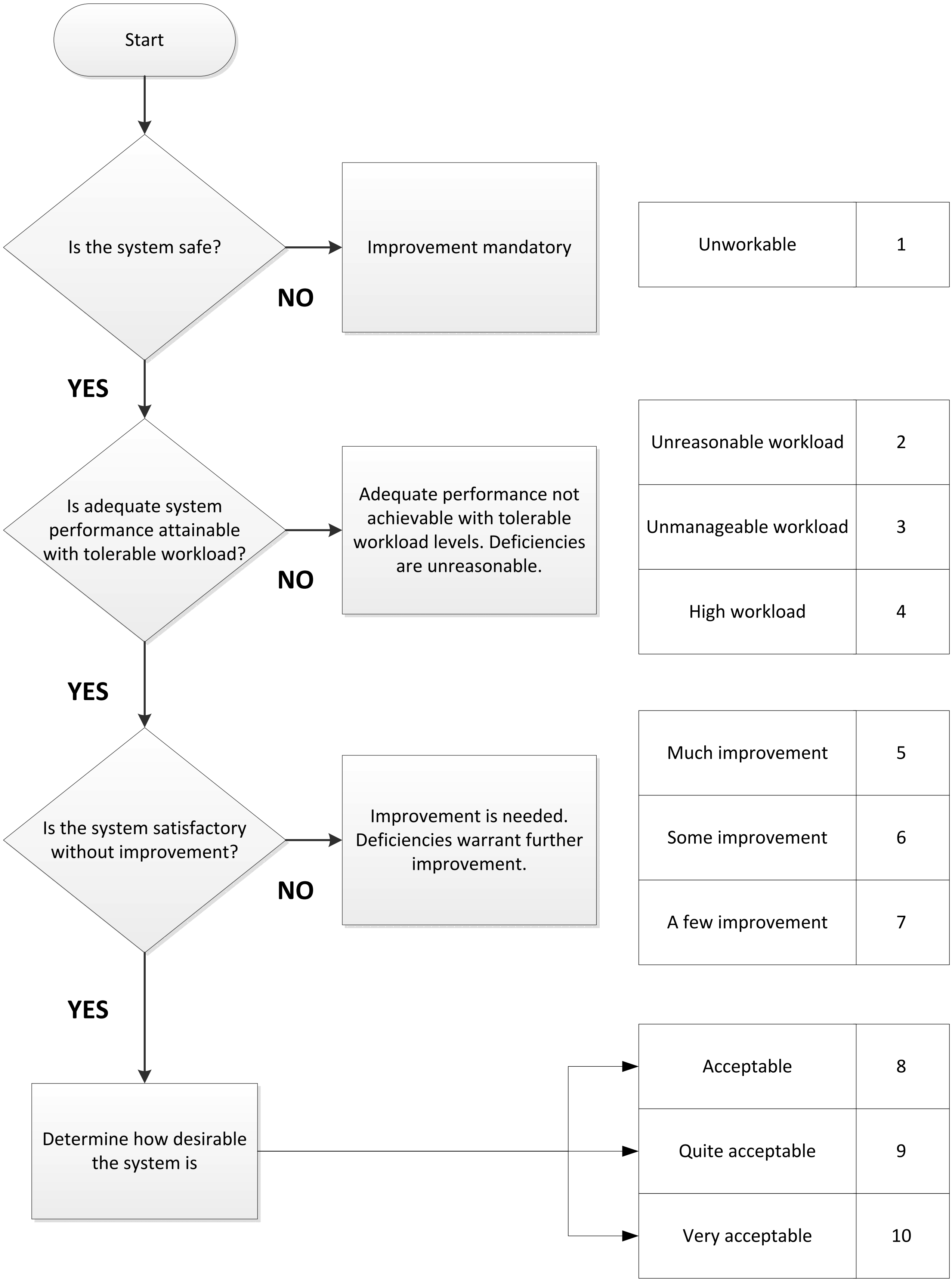

H-2 NASA-TLX Form

NASA Task Load Index (TLX) rating sheet

Subject: Tunnel: Run:

Step 1 Sources of load

☐ Mental demand	☐ Physical demand
☐ Mental demand	☐ Temporal demand
☐ Mental demand	☐ Performance
☐ Mental demand	☐ Effort
☐ Mental demand	☐ Frustration level
☐ Physical demand	☐ Temporal demand
☐ Physical demand	☐ Performance
☐ Physical demand	☐ Effort
☐ Physical demand	☐ Frustration level
☐ Temporal demand	☐ Performance
☐ Temporal demand	☐ Effort
☐ Temporal demand	☐ Frustration level
☐ Performance	☐ Effort
☐ Performance	☐ Frustration level
☐ Effort	☐ Frustration level

Step 2 Magnitude of load

Mental demand

Low High

Physical demand

Low High

Temporal demand

Low High

Performance

Good Poor

Effort

Low High

Frustration level

Low High

NASA TLX rating descriptions

Title	**Endpoints**	**Description**
Mental demand	Low, High	How much mental and perceptual activity was required? (e.g. thinking, deciding, calculating, remembering, looking, searching, etc.) Was the task easy or demanding, simple or complex, exacting or forgiving?
Physical demand	Low, High	How much physical activity was required (e.g. pushing, pulling, turning, controlling, activating, etc.)? Was the task easy or demanding, slow or brisk, slack or strenuous, restful or laborous?
Temporal demand	Low, High	How much time pressure did you feel due to the rate or pace at which the tasks or task elements occured? Was the pace slow and leisurely or rapid and frantic?
Effort	Low, High	How hard did you have to work (mentally or physically) to accomplish your level of performance?
Performance	Good, Poor	How successful do you think you were in accomplishing the goals of the task set by the experimenter (or yourself)? How satisfied were you with your performance in accomplishing these goals?
Frustration Level	Low, High	How insecure, discouraged, irritated, stressed and annoyed versus secure, gratified, content, relaxed and complacent did you feel during the task?

H-3 Web-based Questionnaire

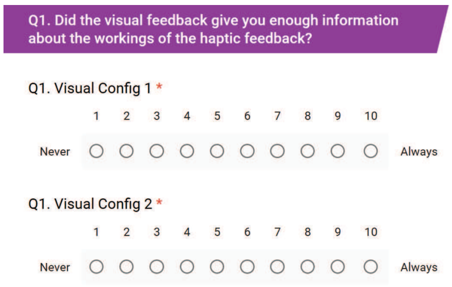
Q1. Did the visual feedback give you enough information about the workings of the haptic feedback?

Q1. Visual Config 1 *

1 2 3 4 5 6 7 8 9 10

Never ○ ○ ○ ○ ○ ○ ○ ○ ○ ○ Always

Q1. Visual Config 2 *

1 2 3 4 5 6 7 8 9 10

Never ○ ○ ○ ○ ○ ○ ○ ○ ○ ○ Always

(a) Rating question 1

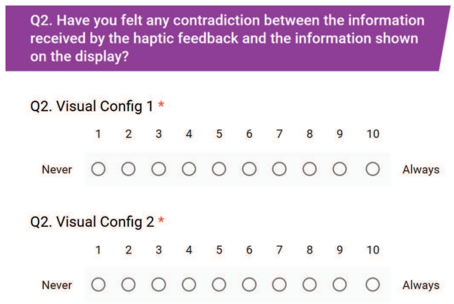
Q2. Have you felt any contradiction between the information received by the haptic feedback and the information shown on the display?

Q2. Visual Config 1 *

1 2 3 4 5 6 7 8 9 10

Never ○ ○ ○ ○ ○ ○ ○ ○ ○ ○ Always

Q2. Visual Config 2 *

1 2 3 4 5 6 7 8 9 10

Never ○ ○ ○ ○ ○ ○ ○ ○ ○ ○ Always

(b) Rating question 2

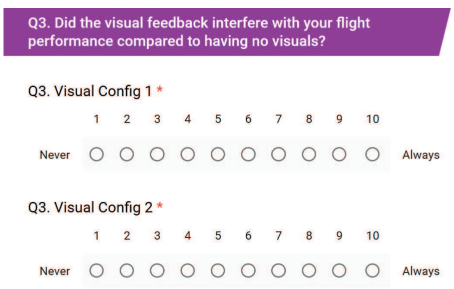
Q3. Did the visual feedback interfere with your flight performance compared to having no visuals?

Q3. Visual Config 1 *

1 2 3 4 5 6 7 8 9 10

Never ○ ○ ○ ○ ○ ○ ○ ○ ○ ○ Always

Q3. Visual Config 2 *

1 2 3 4 5 6 7 8 9 10

Never ○ ○ ○ ○ ○ ○ ○ ○ ○ ○ Always

(c) Rating question 3

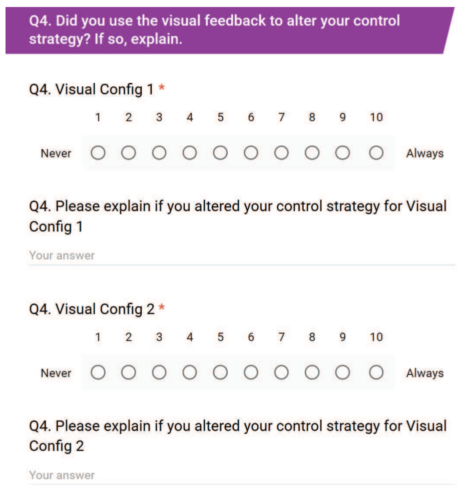
Q4. Did you use the visual feedback to alter your control strategy? If so, explain.

Q4. Visual Config 1 *

1 2 3 4 5 6 7 8 9 10

Never ○ ○ ○ ○ ○ ○ ○ ○ ○ ○ Always

Q4. Please explain if you altered your control strategy for Visual Config 1

Your answer

Q4. Visual Config 2 *

1 2 3 4 5 6 7 8 9 10

Never ○ ○ ○ ○ ○ ○ ○ ○ ○ ○ Always

Q4. Please explain if you altered your control strategy for Visual Config 2

Your answer

(d) Rating question 4 with open question

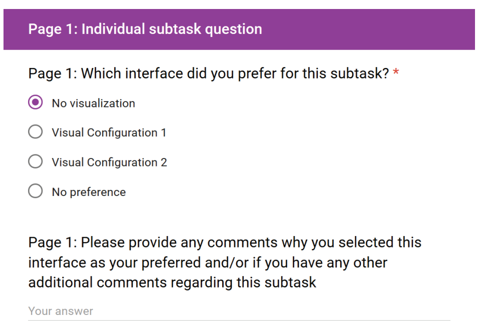
Page 1: Individual subtask question

Page 1: Which interface did you prefer for this subtask? *

- No visualization
- Visual Configuration 1
- Visual Configuration 2
- No preference

Page 1: Please provide any comments why you selected this interface as your preferred and/or if you have any other additional comments regarding this subtask

Your answer

(e) Individual subtask question with open question

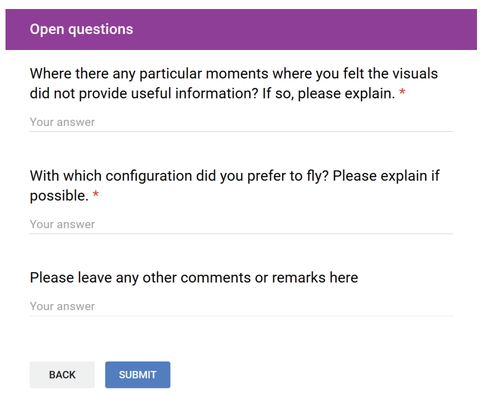
Open questions

Where there any particular moments where you felt the visuals did not provide useful information? If so, please explain. *

Your answer

With which configuration did you prefer to fly? Please explain if possible. *

Your answer

Please leave any other comments or remarks here

Your answer

BACK SUBMIT

(f) Final open questions

H-4 Individual Subtask Questionnaire

These individual subtask questions are given randomly for every participant to minimize the effect of bias. The order in which the questions were presented are shown in table H-1.

Table H-1: Subtask question order

Participant number	Subtask question order
1	2-6-4-3-1-5
2	3-4-6-1-5-2
3	3-2-1-4-6-5
4	5-6-4-3-2-1
5	3-4-5-1-2-6
6	4-6-3-2-5-1
7	5-1-4-2-6-3
8	3-6-5-2-1-4
9	2-5-4-3-6-1
10	4-2-6-5-1-3
11	1-6-4-5-2-3
12	5-2-4-1-6-3

Subtask 1

On-board camera view:

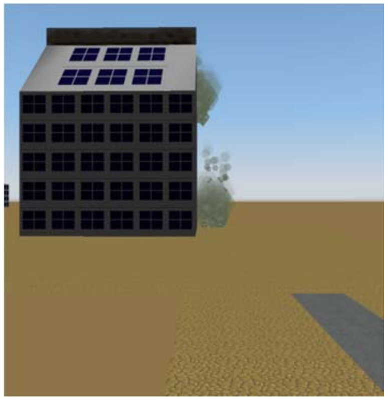

Top view:

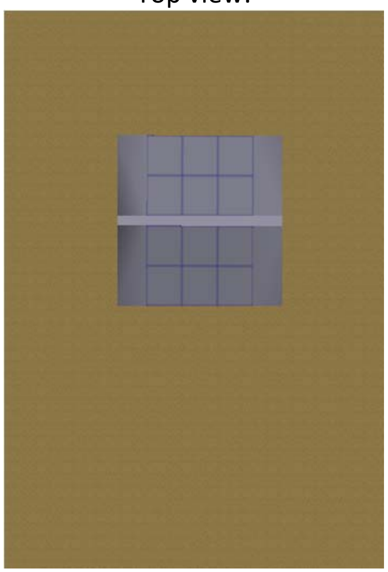

Which interface did you prefer for this subtask?

No Visuals

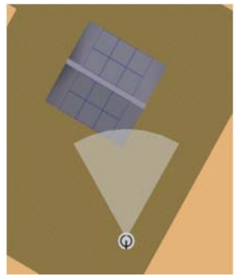

Visual Config 1

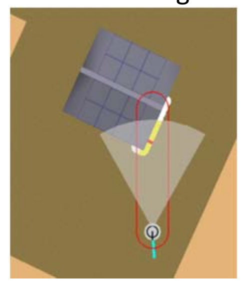

Visual Config 2

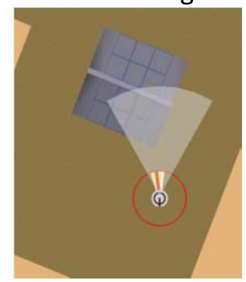

No preference

Please provide any comments why you selected this interface as your preferred and/or if you have any additional comments regarding this subtask

Subtask 2

On-board camera view:

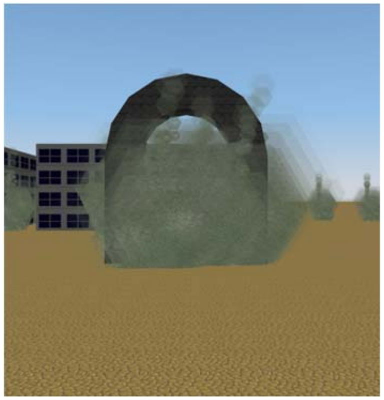

Top view:

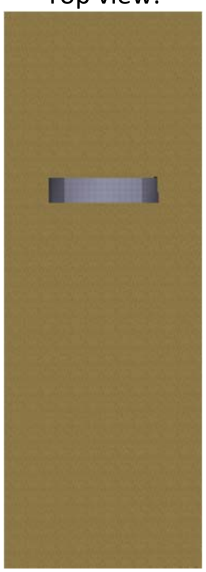

Which interface did you prefer for this subtask?

No Visuals

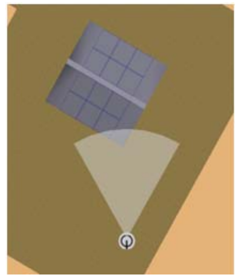

Visual Config 1

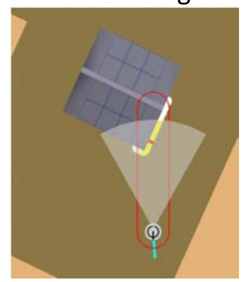

Visual Config 2

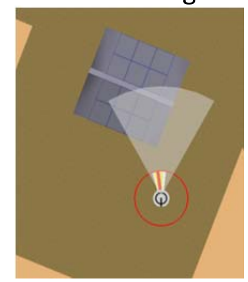

No preference

Please provide any comments why you selected this interface as your preferred and/or if you have any additional comments regarding this subtask

Subtask 3

On-board camera view:

Top view:

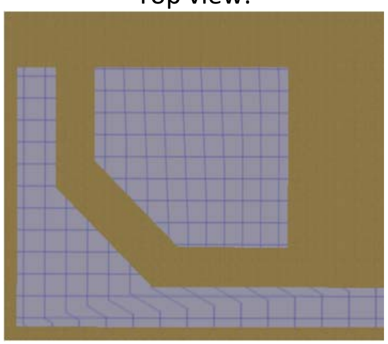

Which interface did you prefer for this subtask?

No Visuals

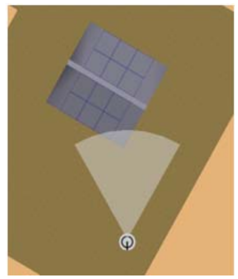

Visual Config 1

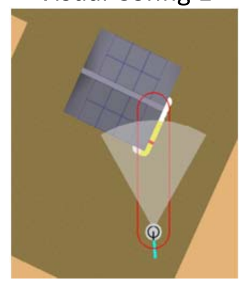

Visual Config 2

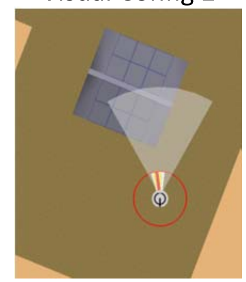

No preference

Please provide any comments why you selected this interface as your preferred and/or if you have any additional comments regarding this subtask

Subtask 4

On-board camera view:

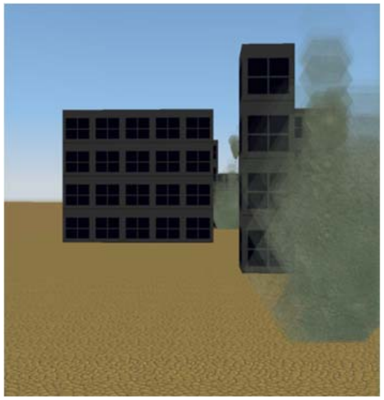

Top view:

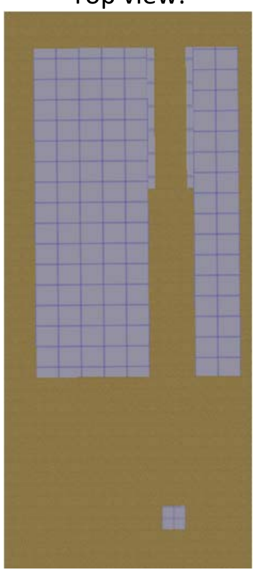

Which interface did you prefer for this subtask?

No Visuals

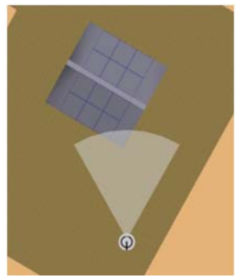

Visual Config 1

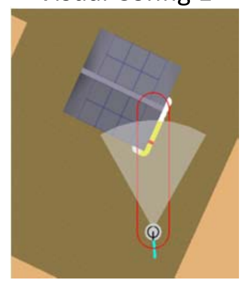

Visual Config 2

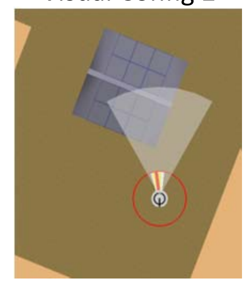

No preference

Please provide any comments why you selected this interface as your preferred and/or if you have any additional comments regarding this subtask

Subtask 5

On-board camera view:

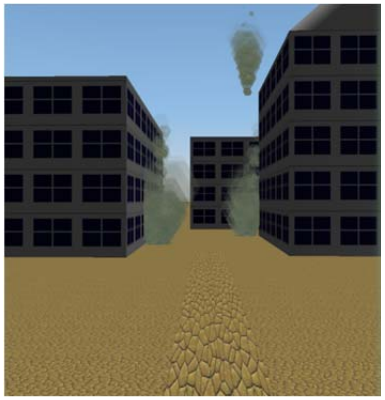

Top view:

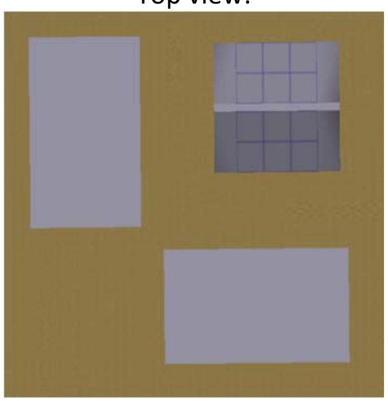

Which interface did you prefer for this subtask?

No Visuals

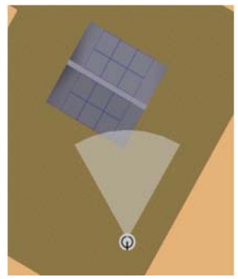

Visual Config 1

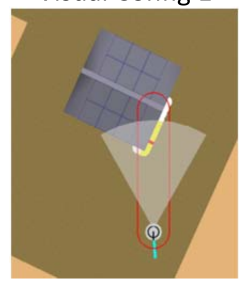

Visual Config 2

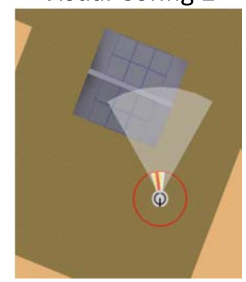

No preference

Please provide any comments why you selected this interface as your preferred and/or if you have any additional comments regarding this subtask

Subtask 6

On-board camera view:

Top view:

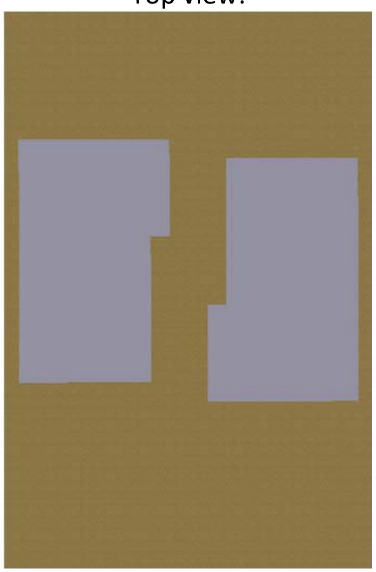

Which interface did you prefer for this subtask?

No Visuals

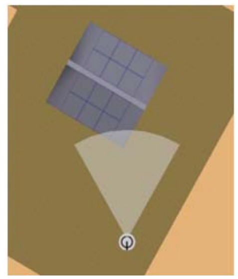

Visual Config 1

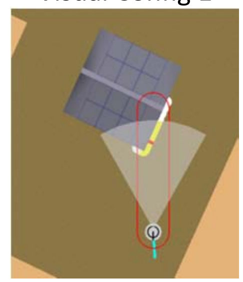

Visual Config 2

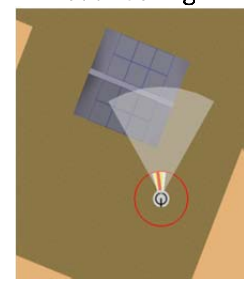

No preference

Please provide any comments why you selected this interface as your preferred and/or if you have any additional comments regarding this subtask

Appendix I

Additional Evaluations Results

This chapter provides additional results of the experiment that are not presented in the scientific paper.

In the scientific paper, the control activity and haptic activity had the results of the x and y output. The resultant of these outputs, $\sigma_{\dot{\delta}_{st}}$ standard deviation stick rate $[rad/s]$, $\bar{M}_{NMS}$ mean neuromuscular moment $[Nm]$ and $\bar{M}_{Hap}$ mean haptic moment $[Nm]$, can be seen respectively in section I-1.

The paper presented the subjective ratings for the NASA-TLX. Additionally calculated Z-scores of the questionnaire are presented in section I-2. Also for the Likert scale questions which are plotted as boxplots in the paper, are shown alternatively as frequency plots in section I-3.

After the human-in-the-loop experiment, several open questions were filled in by the participants. The answers are noted in section I-4. The participants used names like configuration 1 for (PRF-CRF) and configuration 2 for (SCRF).

I-1 Additional Resultant Measurements

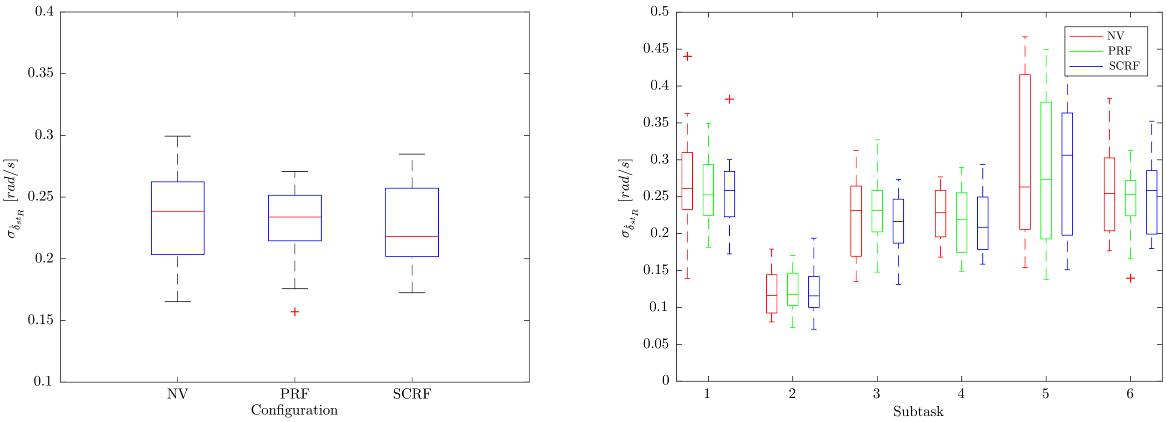

(a) Configuration overall **(b)** Subtask specific

Figure I-1: Resultant standard deviation side-stick deflection rate box plots for both configuration and subtask separately

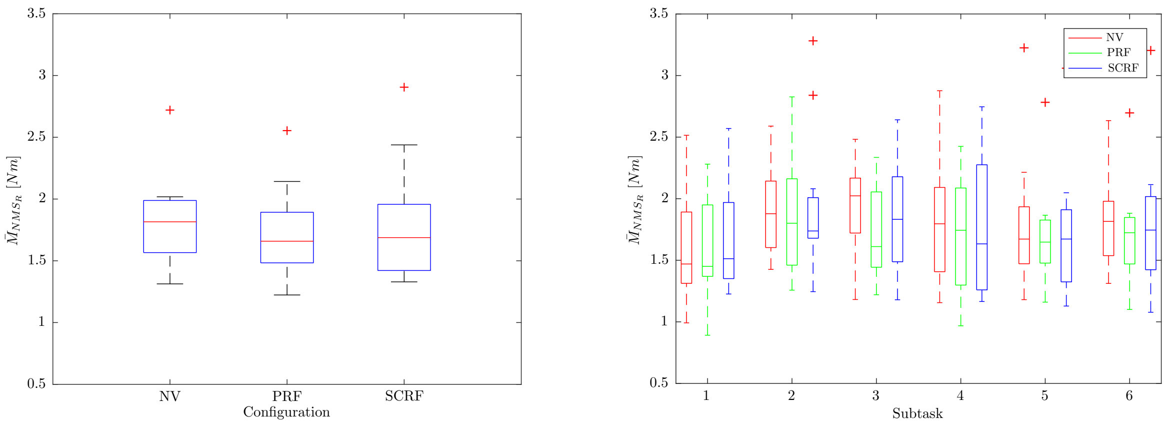

(a) Configuration overall **(b)** Subtask specific

Figure I-2: Resultant mean neuromuscular moment box plots for both configuration and subtask separately

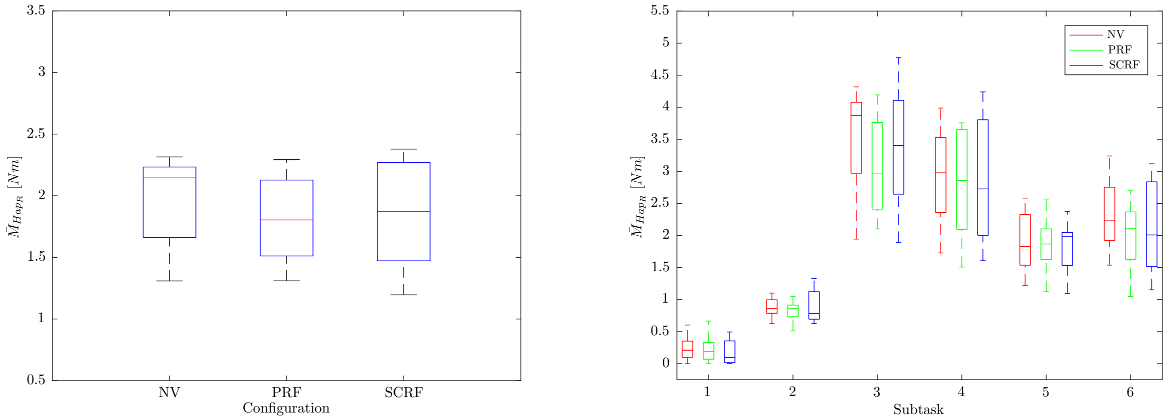

(a) Configuration overall **(b)** Subtask specific

Figure I-3: Resultant mean haptic moment box plots for both configuration and subtask separately

I-2 NASA TLX Z-Scores

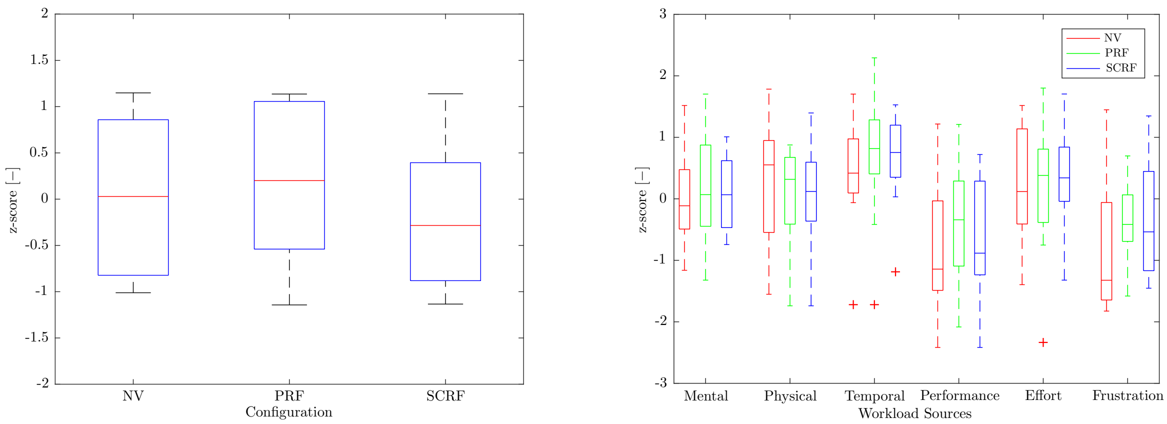

(a) Overall rating **(b)** Rating for specific sources

Figure I-4: NASA TLX z-scores

I-3 Rating Scale Questions Frequency Plots

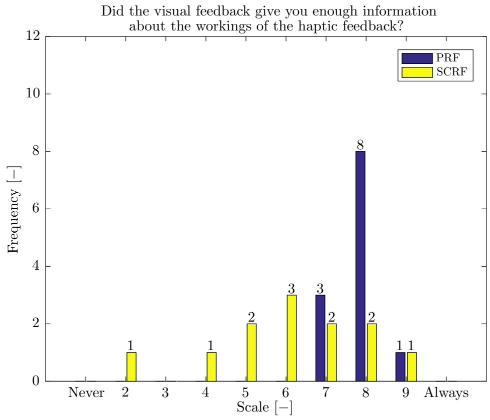

(a) Question 1

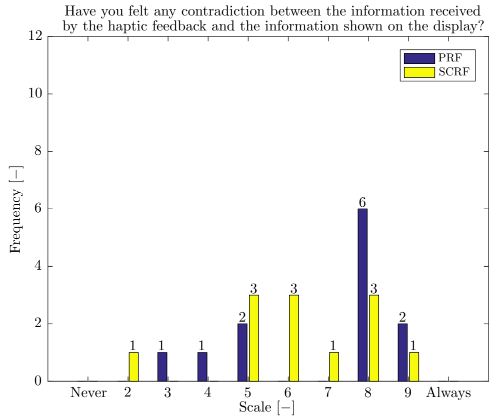

(b) Question 2

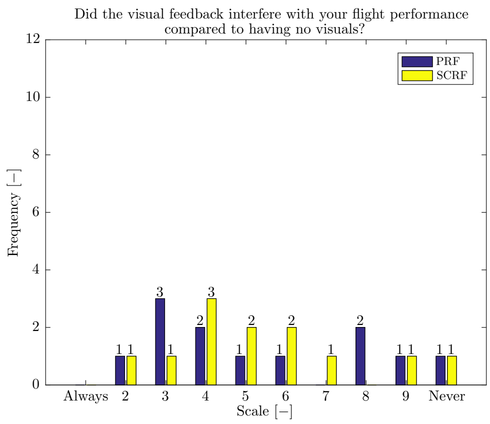

(c) Question 3

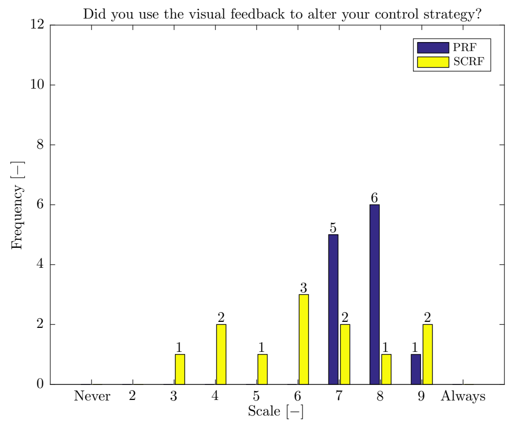

(d) Question 4

Figure I-5: Scaling question frequency plots from questionnaire

I-4 Open Question Answers

Table I-1: Rating question 4 open answer (Did you use the visual feedback to alter your control strategy?)

Par. nr.	Configuration PRF-CRF	Configuration SCRF
1	Ability to fly much closer to objects	Ability to fly closer to objects, and more precision
2	I altered my control strategy by comparing the obstacle colors and by trying to have the same color left and right.	I altered my control strategy by trying to point the red obstacle indicator parallel to the obstacles.
3	Used the visual feedback to get a more detailed overview of distance with respect to the building. Especially configuration 1 was useful, using the additional red color.	Used the visual feedback to get a more detailed overview of distance with respect to the building. Missed and indication of how close to the buildings as in config 1
4	Use the vector to determine when to slow down and to speed up	Did go much slower
5	I took more risk	I took more risk
6	more cautious for collisions, slower	-
7	With visual feedback, I 'listened' better to the haptic feedback. Also, the red contour allowed for better planning of the trajectory along a wall and in the forward direction.	With visual feedback I 'listened' better to the haptic feedback. Also in the forward motion, slowing down a bit.
8	I was able to take corners more narrow due to early warnings.	As here I got more early warnings due to the combination of visual and haptics. Therefore I think that I was able to take corners faster. Also for 1 and 2, I think I looked more at the navigation display than when I didn't have feedback (config 0)
9	Steered closer to the wall because it was clear how close you could get	Steered towards the red vector in the close spaces
10	I lowered my speed and tried harder to avoid the visual bar to become red.	I tried to avoid switching the vector from going from left to right, since I wanted to avoid the haptic feedback to influence my flight between the narrow part of the circuit.
11	With this visual, I could use the red speed contour for my control strategy. I made sure the speed contour did not cross any walls, then I would not receive any haptic feedback and I could maintain a high speed.	No, with this visual I did not alter my strategy
12	Used it in narrow pathways to steer clear of the edges, and to optimize speed	Used it in narrow pathways to steer clear of the edges

Table I-2: Individual Subtask 1 Question (Please provide any comments why you selected this interface as your preferred and/or if you have any additional comments regarding this subtask.)

Par. nr.	Pref. Choice	Answer
1	SCRF	Again, maintain velocity and cut to the corner
2	No Pref.	Used on-board camera to fly in a straight line
3	PRF-CRF	Get a better overview of your location with respect to the building. Especially the red indicator was useful to see if you are to close to the building
4	PRF-CRF	-
5	PRF-CRF	In order to get as fast as possible to the second plume, Visual config 1 was very helpful in making the sharp turn
6	No Visual	Without visual you can see how far you are from the corner
7	PRF-CRF	The red contour allowed for better trajectory planning.
8	PRF-CRF	Here vis config 1 lagged less than for the other subtasks. It proved to be useful since the corner was indicated more clearly. than for vis config2 or no vis.
9	PRF-CRF	You had to slow down a lot to get the second plume. The size of the contour really helped. Furthermore it was very clear how close you were next to the corner
10	SCRF	-
11	PRF-CRF	When approaching the building, visual 1 helped me to go parallel to the building without receiving (delaying) haptic feedback.
12	PRF-CRF	best for drifting through the corner

Table I-3: Individual Subtask 2 Question (Please provide any comments why you selected this interface as your preferred and/or if you have any additional comments regarding this subtask.)

Par. nr.	**Pref. Choice**	**Answer**
1	SCRF	Better overview
2	PRF-CRF	Config 1 useful to determine you location with respect to the corners. Used this to fly more through the smoke.
3	No Pref.	Also used on-board camera view for the gate
4	No Pref.	Easy to do without any help
5	No Visual	The gate was not that small, so no additional visual feedback was needed
6	No Pref.	-
7	No Pref.	Full speed!
8	SCRF	Was easy enough. But with 2 it was even more easy to get the plume exactly in the middle.
9	PRF-CRF	Thanks to the white/yellow/red color it was clear on which side you were too close
10	No Pref.	I used the onboard camera view for this task.
11	PRF-CRF	For the gate, visual 1 was very helpful. With this display, my strategy was to steer the speed contour between the two pillars of the gate, such that I did not get haptic feedback. This was an added value of visual 1, not so much of visual 2 or no visualization.
12	No Pref.	port is closed on navigation map

Table I-4: Individual Subtask 3 Question (Please provide any comments why you selected this interface as your preferred and/or if you have any additional comments regarding this subtask.)

Par. nr.	Pref. Choice	Answer
1	SCRF	Fast feedback of environment, ability to go fast and close to the corners
2	No Pref.	Used on-board camera view to navigate
3	No Pref.	Used on-board camera view to navigate
4	No Pref.	Only looked at the vehicle circle
5	No Visual	Haptic feedback was decent
6	SCRF	short radius helped with wall distance detection, config 1 made me dougt my actual location wrt wall
7	No Visual	There was plenty of space to maneuver. Therefore i overruled the haptic feedback a lot, and visualization was only distraction.
8	SCRF	Provided more feedback than no visualisation, and was not lagging due to CPU overload as config 1.
9	PRF-CRF	Was clear how much margin you had on each side. The size of the red contour helped with assessing the speed
10	No Visual	The haptic visuals were more annoying than useful for this part, so I prefer no visual haptics for this task.
11	PRF-CRF	Here I liked the white-orange-red indication on the walls (visual 1), which helped me to stay clear of all walls. I missed this with other visualizations.
12	PRF-CRF	gives good information about how to take the corner, not too much information centered

Table I-5: Individual Subtask 4 Question (Please provide any comments why you selected this interface as your preferred and/or if you have any additional comments regarding this subtask.)

Par. nr.	Pref. Choice	Answer
1	SCRF	This was the most difficult for me, a glance on config 2 allowed me to be sure that I was in the middle
2	No Pref.	Also used on-board camera view for the gate
3	No Pref.	Used on-board camera to fly in a straight line
4	PRF-CRF	Used the speed vector to keep the vehicle in the middle
5	PRF-CRF	The white, yellow and red blocks were really helpful before going into the narrowest part, however in here I just used the haptic feedback
6	SCRF	short radius helped with wall distance detection, config 1 made me dougt my actual location wrt wall
7	PRF-CRF	Since visual feedback was given for a greater part of the planned trajectory, this allowed for averaging the left and right boundary better than configuration 2.
8	SCRF	2 was better for two reasons: 1. No lagging. 2. Also since the visuals extent from your own UAV, you were 'drawn' into the narrow part, so I was able to do this task quicker.
9	PRF-CRF	Config 1 had my preference, but config 2 was also okay. You could use the red vector in the middle of the corridor.
10	SCRF	In my opinion config 1 was very annoying for this task. It felt if the spacing between two buildings was even more narrow because of the white visual haptic feedback system. The second config was the best option for me since it gave me less stress during the tasks.
11	No Visual	The visuals did not really help here, mainly because my perception of the haptic feedback was different from what the visuals were telling me. In fact, the haptic feedback was a bit of an annoyance here, because it kept pushing me back and forth while I tried to get through the buildings. Visuals cluttered the display a little bit.
12	SCRF	visualization 1 gives to much distraction on the sides of the wall, no visualization gives no indication about your vector

Table I-6: Individual Subtask 5 Question (Please provide any comments why you selected this interface as your preferred and/or if you have any additional comments regarding this subtask.)

Par. nr.	Pref. Choice	Answer
1	SCRF	-
2	PRF-CRF	Useful to determine your location with respect to the corners. On-board camera didn't provide enough information, but the top view did. Preferred config 1 since it gave a clear indication of approaching the building too close.
3	PRF-CRF	Config 1 useful to determine you location with respect to the corners. Used this to fly more through the smoke.
4	PRF-CRF	Use the speed vector for the direction
5	No Visual	-
6	PRF-CRF	long smooth trajectory along wall, estimation to the wall was nice to plan your trajectory
7	No Visual	Since the smoke was close to the corner, without visual feedback i focused more on the situation. With visualization, I was focusing more on why the haptic feedback was given than my exact location and situation.
8	SCRF	Not really a preference for 1 or 2, but for the second plume it was handy to get more feedback.
9	PRF-CRF	Thanks to the white/yellow/red color it was clear on which side you were too close
10	SCRF	It was easier to fly next to the corners of the building (especially for the outer corner).
11	PRF-CRF	Similar to subtask 1, visual 1 helped me to steer parallel to the building when approaching the subtask. This helped to complete the task more quickly. The other display did not help me with this.
12	PRF-CRF	has more preview

Table I-7: Individual Subtask 6 Question (Please provide any comments why you selected this interface as your preferred and/or if you have any additional comments regarding this subtask.)

Par. nr.	**Pref. Choice**	**Answer**
1	SCRF	-
2	PRF-CRF	Get a better overview of your location with respect to the building. Especially the red indicator was useful to see if you are to close to the building
3	PRF-CRF	Useful to determine your location with respect to the corners. On-board camera didn't provide enough information, but the top view did. Preferred config 1 since it gave a clear indication of approaching the building too close.
4	No Visual	-
5	PRF-CRF	This task requires you to make some sharp turns. The guidance with the red speed vector and the white, yellow and red blocks was useful
6	No Visual	-
7	PRF-CRF	-
8	PRF-CRF	Even while there was cpu overload, I could better see the "seriousness" of the corners of the building, so I was able to come closer to the plumes more easily.
9	PRF-CRF	Was clear how much margin you had on each side. The size of the red contour helped with assessing
10	SCRF	In my opinion config 1 was very annoying for this task. It felt if the spacing between two buildings was even more narrow because of the white visual haptic feedback system. The second config was the best option for me since it gave me less stress during the tasks.
11	PRF-CRF	The speed contour helped me to steer right between the two buildings. The other visuals did not help me very much with this.
12	No Pref.	-

Table I-8: Open Question 1 (Where there any particular moments where you felt the visuals did not provide useful information? If so, please explain.)

Par. nr.	Answer
1	Both visuals were useful for me, especially when flying close to an obstacle. Visual 1 was laggy sometimes, such that there seemed to be a delay between the visual feedback, and the current velocity and position with respect to the obstacles.
2	For straight flight with no obstacles near, the visuals do not provide useful information. For some obstacles, it increased the performance (i.e. the narrow alley) and for some it increased the complexity of the task (i.e. the 90 degree corner).
3	No, all the times the visuals gave a clear indication where your position was relative to the buildings and when flying too close to the buildings.
4	Config 2 confused me, since I could not follow any line
5	Visual config 1: I did not really notice the blue vector; Visual config 2: the visual degradations were to small to improve my performance
6	open areas
7	The blue haptic feedback indication was useless. At least, i didn't use it;)
8	Yes, when it was lagging. When the navigation display was lagging and the visuals in front were not, it was easier to follow the big screen.
9	no
10	For the second configuration the switching of the red vector was sometimes later than the haptic feedback system itself. There is a possibility that I needed to correct more because of this. The first configuration was giving me too much information. Because of this I looked less on the onboard view display.
11	I found visual 2 a bit confusing, some of the information was not very useful. For visual 1, all information was useful.
12	in the portal visuals were useless, in the small corridor visuals were sometimes too crowded

Table I-9: Open Question 2 (With which configuration did you prefer to fly? Please explain if possible.)

Par. nr.	Answer
1	I have a very clear preference for configuration 2, as for me it provides all the information in a more compact form, which is faster to perceive when quickly looking down. Also when focussing only on the top down view, I found configuration 2 was better. I think configuration 1 was not optimal, since there seemed to be some "laggy" effects, with the visual feedback struggling to keep up with the current situation. This contributed only slightly for my preference of configuration 2.
2	Configuration 1. Since it shows the most useful information overall. Although it doesn't provide useful information for all subtasks.
3	Config 1. I liked the contour line and the red indicator of flying too close to the buildings
4	Config 1, the speed vector is very helpfull
5	In most cases no visual feedback was also fine, even in narrow sharp paths. However, when some special turns, especially the sharp ones, are needed, Visual config 1 was preferable!
6	config 2, short range help
7	Configuration 1: I liked the red contour for short-term trajectory planning. And this was the clearest configuration for displaying what caused the haptic feedback.
8	With config2. I think if the PC was not lagging, I would have prefered visual 1. For both visuals, it is more easy to see for what obstacle the haptic feedback is actually warning you for. However, for easy subtasks, I might prefer visual 1, since it was not lagging as much and provided an earlier warning.
9	config 1. Was very clear on how close you were wrt to the side and the size of the red contour helped with assessing your speed
10	Configuration 2 since this system was giving useful information without being distracted much from the onboard display. It was more easier to detect the haptic feedback system. Less force was needed to control this system during the tasks.
11	I preferred visual 1, because it helped me to understand the haptic feedback better. With this understanding, I was able to reduce the amount of 'push-back' I received from the haptic feedback, by making sure the speed contour did not overlap with any buildings.
12	visual configuration 1. gave clear information about your speed and obstacles but the information was not too centered

Table I-10: Open Question 3 (Please leave any other comments or remarks here.)

Par. nr.	Answer
1	What I found really frustrating is the Haptic feedback, particularly when flying straight on to an obstacle, and having to force the stick forward, while I was sure no collision would occur. I feel that the side forces for haptic feedback are far more relevant.
2	The haptic feedback on its own already provides a lot of useful information on obstacle collision risk. The visual aids can increase the performance, but they increase the mental load as well.
3	Mostly related to the feedback: Sometimes it was a little to strong for my taste. The visual configuration was really nice and useful, especially when the on-board camera didn't provide enough information (tight corners)
4	-
5	I have the tendancy to take more risk if visual feedback is provided
6	haptic feedback vector never used, only wall detection/ distance to wall was usefull in the visual
7	-
8	I think the experiment was done in a professional way. Kudo's :)!
9	In the tight corridor the stick shook a lot back and forth when you were exactly in the middle. This very annoying and tiresome to steer.
10	For configuration 2 the white bars felt sometimes as walls during flight. It would be better to add some transparency to these bars to have a more natural feeling of the system. The speed ellipse of system 1 was not very useful to me.
11	The visuals, and particularly visual 1, did help me to better understand the haptic feedback. Overall, I sometimes found the haptic feedback a bit of an annoyance, particularly when trying to steer between two buildings. I felt the haptic feedback slowed me down. The visuals particularly helped to better understand the haptic feedback and reduce the adverse effects of 'push-back' of the haptic feedback.
12	in small corridor the haptic feedback was useless

Bibliography

Borst, C., Grootendorst, F. H., Brouwer, D. I. K., Bedoya, C., Mulder, M., & Paassen, M. M. van. (2014). Design and Evaluation of a Safety Augmentation System for Aircraft. *J. Aircr.*, *51*(1), 12–22.

Hart, S. G., & Staveland, L. E. (1988). Development of NASA-TLX (Task Load Index) - Results of Empirical and Theoretical Research. *Adv. Psychol.*, *52*(C), 139–183.

Kolsteeg, J. M., Smisek, J., Paassen, M. M. van, & Mulder, M. (2014). Haptic Interface for UAV Teleoperation - Changing Haptic Control Device Stifness based on Environmental Constraints. *TU Delft, Unpubl.*, 1–15.

Kuchar, J. K., & Drumm, A. C. (2007). The Traffic Alert and Collision Avoidance System. *Lincoln Lab. J.*, *16*(2), 277–296.

Lam, T. M. (2009). *Haptic Interface for UAV Teleoperation.* Doctoral dissertation, Delft University of Technology.

Lam, T. M., Boschloo, H. W., Mulder, M., Paassen, M. M. van, & Helm, F. C. T. van der. (2004). Effect of Haptic Feedback in a Trajectory Following Task with an Unmanned Aerial Vehicle. *2004 IEEE Int. Conf. Syst. Man Cybern.*, *3*, 2500–2506.

Lee, K. K. (2001). Development and Validation of the Controller Acceptance Rating Scale (CARS). *4th USA/Europe Air Traffic Manag. R&D Semin.*, 14.

Parasuraman, R., & Riley, V. (1997). Humans and Automation: Use, Misuse, Disuse, Abuse. *Hum. Factors*, *39*, 230–253.

Parasuraman, R., Sheridan, T. B., & Wickens, C. D. (2008, jul). Situation Awareness, Mental Workload, and Trust in Automation: Viable, Empirically Supported Cognitive Engineering Constructs. *J. Cogn. Eng. Decis. Mak.*, *2*(2), 140–160.

Parasuraman, R., & Wickens, C. D. (2008). Humans: Still Vital After All These Years of Automation. *Hum. Factors Ergon. Soc.*, *50*(3), 511–520.

Seppelt, B. D., & Lee, J. D. (2007). Making adaptive cruise control (ACC) limits visible. *Int. J. Hum. Comput. Stud.*, *65*(3), 192–205.

Sunil, E., Smisek, J., Paassen, M. M. van, & Mulder, M. (2014). Tuning of a Haptic Collision Avoidance System for Unmanned Aircraft Teleoperation. *TU Delft, Unpubl.*, 1–24.

Wickens, C. D., Dixon, S. R., & Ambinder, M. S. (2006). Workload and Automation Reliability in Unmanned Air Vehicles. *Hum. Perform. Cogn. Eng. Res.*, *7*, 209–222.

Wickens, C. D., Lee, J., Liu, Y., & Becker, S. G. (2004). *An Introduction to Human Factors Engineering* (Second Edi ed.). New Jersey: Pearson.